Cell Reports

Article

GDF15 mediates the metabolic effects of PPARβ/δ by activating AMPK

Graphical abstract

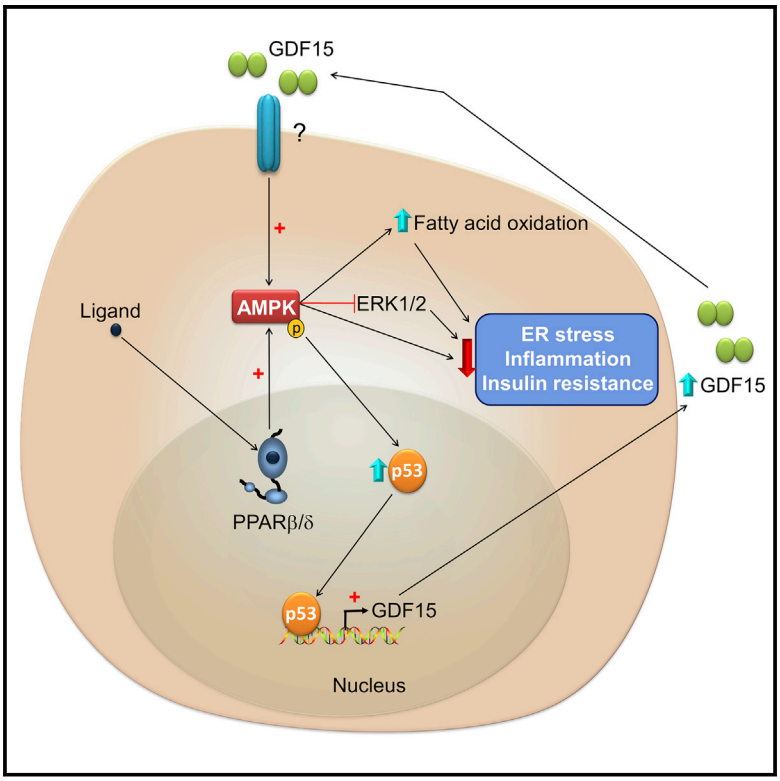

Authors

David Aguilar-Recarte, Emma Barroso, Anna Gumà, ..., Xavier Palomer, Walter Wahli, Manuel Vázquez-Carrera

Correspondence

mvazquezcarrera@ub.edu

In brief

GDF15 is a stress response cytokine that regulates energy metabolism. Aguilar-Recarte et al. show that PPARβ/δ activation increases GDF15 levels, which contributes to the metabolic effect of this receptor and activates AMPK in skeletal muscle independently of GDF15 receptor GFRAL.

Highlights

- Activation of the AMPK-p53 pathway by PPARβ/δ agonists increases GDF15
- Many metabolic effects mediated by PPARβ/δ activation are abrogated in *Gdf15*$^{-/-}$ mice
- GDF15 is required for the activation of AMPK by ligand-activated PPARβ/δ
- In skeletal muscle, GDF15 activates AMPK in the absence of the GDF15 receptor GFRAL

Aguilar-Recarte et al., 2021, Cell Reports *36*, 109501
August 10, 2021
https://doi.org/10.1016/j.celrep.2021.109501

CellPress

Cell Reports

CellPress
OPEN ACCESS

Article

GDF15 mediates the metabolic effects of PPARβ/δ by activating AMPK

David Aguilar-Recarte,[1,2,3,4] Emma Barroso,[1,2,3,4] Anna Gumà,[2,3,5] Javier Pizarro-Delgado,[1,2,3,4] Lucía Peña,[1,2,3,4] Maria Ruart,[1,2,3,4] Xavier Palomer,[1,2,3,4] Walter Wahli,[6,7,8] and Manuel Vázquez-Carrera[1,2,3,4,9,*]

[1]Department of Pharmacology, Toxicology and Therapeutic Chemistry, Faculty of Pharmacy and Food Sciences, University of Barcelona, 08028 Barcelona, Spain

[2]Institute of Biomedicine of the University of Barcelona (IBUB), University of Barcelona, 08028 Barcelona, Spain

[3]Spanish Biomedical Research Center in Diabetes and Associated Metabolic Diseases (CIBERDEM)-Instituto de Salud Carlos III, 28029 Madrid, Spain

[4]Pediatric Research Institute-Hospital Sant Joan de Déu, 08950 Esplugues de Llobregat, Spain

[5]Department of Biochemistry and Molecular Biomedicine, Faculty of Biology, University of Barcelona, 08028 Barcelona, Spain

[6]Center for Integrative Genomics, University of Lausanne, 1015 Lausanne, Switzerland

[7]Lee Kong Chian School of Medicine, Nanyang Technological University Singapore, Singapore 308232, Singapore

[8]ToxAlim (Research Center in Food Toxicology), INRAE, UMR1331, 31300 Toulouse Cedex, France

[9]Lead contact

*Correspondence: mvazquezcarrera@ub.edu

https://doi.org/10.1016/j.celrep.2021.109501

SUMMARY

Peroxisome proliferator-activated receptor β/δ (PPARβ/δ) activates AMP-activated protein kinase (AMPK) and plays a crucial role in glucose and lipid metabolism. Here, we examine whether PPARβ/δ activation effects depend on growth differentiation factor 15 (GDF15), a stress response cytokine that regulates energy metabolism. Pharmacological PPARβ/δ activation increases GDF15 levels and ameliorates glucose intolerance, fatty acid oxidation, endoplasmic reticulum stress, and inflammation, and activates AMPK in HFD-fed mice, whereas these effects are abrogated by the injection of a GDF15 neutralizing antibody and in *Gdf15*$^{-/-}$ mice. The AMPK-p53 pathway is involved in the PPARβ/δ-mediated increase in GDF15, which in turn activates again AMPK. Consistently, *Gdf15*$^{-/-}$ mice show reduced AMPK activation in skeletal muscle, whereas GDF15 administration results in AMPK activation in this organ. Collectively, these data reveal a mechanism by which PPARβ/δ activation increases GDF15 levels via AMPK and p53, which in turn mediates the metabolic effects of PPARβ/δ by sustaining AMPK activation.

INTRODUCTION

Growth differentiation factor 15 (GDF15) is a cytokine that has been implicated in multiple biological processes, including the regulation of energy homeostasis (Tsai et al., 2018). This distant member of the transforming growth factor β (TGF-β) superfamily acts as a cell stress-response factor and is expressed in several organs, including the liver, skeletal muscle, adipose tissue, kidney, and placenta (Hromas et al., 1997; Paralkar et al., 1998; Fairlie et al., 1999; Ding et al., 2009). Its expression is upregulated following injury, mitochondrial dysfunction, inflammation, and cancer by the action of several transcription factors, including p53 (Kannan et al., 2000; Li et al., 2000; Tan et al., 2000; Osada et al., 2007), early growth response 1 (egr-1) (Baek et al., 2004; 2005), and C/EBP homologous protein (CHOP) (Chung et al., 2017). Normal circulating levels of GDF15 range between 100 and 1,200 pg/mL, increasing after exercise and in many disease processes (Tsai et al., 2018).

GDF15 plays a crucial role in metabolism, mainly through its neuronal receptor, glial-derived neurotrophic factor (GNDF) receptor α-like (GFRAL) (Tsai et al., 2018). Thus, administration of GDF15 in obesity improves glucose tolerance by reducing food intake (Emmerson et al., 2017; Yang et al., 2017; Mullican et al., 2017; Hsu et al., 2017). In addition, transgenic mice overexpressing *Gdf15* show a lean phenotype and a reduction in food intake and are more resistant to obesity, metabolic inflammation, and glucose intolerance (Johnen et al., 2012; Macia et al., 2012; Chrysovergis et al., 2014; Wang et al., 2014a, 2014b). These findings indicate that the effects of GDF15 occur via GFRAL-dependent anorexic actions in the brain. However, this cytokine also increases thermogenesis, lipid catabolism, and mitochondrial oxidative phosphorylation independently of changes in food intake (Chung et al., 2017), suggesting that GDF15 might also exert its effects via other so far unknown receptors.

The nuclear receptor peroxisome proliferator-activated receptor β/δ (PPARβ/δ) regulates glucose and lipid metabolism, as well as inflammation. Consequently, the activation of PPARβ/δ by agonists attenuates dyslipidemia and hyperglycemia, improves whole-body insulin sensitivity, and prevents diet-induced obesity (Vázquez-Carrera 2016; Tan et al., 2016). Many of the anti-inflammatory and antidiabetic effects of PPARβ/δ activation in skeletal muscle, including the reduction of endoplasmic

reticulum (ER) stress and the prevention of lipid-induced activation of the pro-inflammatory nuclear factor (NF)-κB pathway, are dependent on AMP-activated protein kinase (AMPK) activation (Coll et al., 2010; Salvadó et al., 2014). Likewise, the administration of PPARβ/δ ligands to mice fed a high-fat diet (HFD) increases fatty acid oxidation through AMPK activation in the liver, resulting in glucose-lowering activity (Lee et al., 2006; Barroso et al., 2011; Bojic et al., 2014). However, it is not known whether these metabolic effects of PPARβ/δ ligands involve GDF15, a key factor in metabolism. In the present study, we show that PPARβ/δ activation induces GDF15 levels through an AMPK-p53-dependent mechanism, and in turn, GDF15 sustains AMPK activity and is necessary for the beneficial effects of PPARβ/δ ligands on glucose intolerance, ER stress, and inflammation in HFD-fed mice.

RESULTS

In skeletal muscle, GDF15 neutralization reverts the beneficial effects of PPARβ/δ activation on lipid metabolism, ER stress, inflammation, and insulin signaling

Treatment of C2C12 myotubes with the PPARβ/δ agonist GW501516 for 12, 18, and 24 h significantly increased mRNA and protein levels of GDF15 and its secretion into the culture media (Figures S1A–S1C). This effect of GW501516 was specifically dependent on PPARβ/δ because the PPARβ/δ antagonist GSK3787 or knockdown of the receptor by small interfering RNA (siRNA) transfection attenuated the increase in *Gdf15* expression (Figures S1D–S1F). Similarly, mice treated with GW501516 for 2, 4, and 6 days showed that only in the latter duration *Gdf15* expression was increased in skeletal muscle (Figure S1G). This was accompanied by enhanced GDF15 protein levels in skeletal muscle and serum (Figures S1H and S1I). A different PPARβ/δ agonist, GW0742, also increased GDF15 protein levels in skeletal muscle (Figure S1J), indicating that the effect observed for GW501516 was not limited only to this specific ligand.

Next, we evaluated whether the effects of the PPARβ/δ ligand GW501516 on HFD-fed mice depended on GDF15 by using GDF15 neutralizing antibody or immunoglobulin G (IgG) as control. Importantly, the dose of the neutralizing antibody used attenuated the reduction in food intake caused by recombinant mouse GDF15 (Figure S2), demonstrating that the antibody effectively blocked the GDF15 effects. GW501516 improved glucose intolerance in HFD-fed mice, but this beneficial effect was inhibited by the GDF15 neutralizing antibody (Figures 1A and 1B). Importantly, neither GW501516 nor antibody treatment affected food intake or body weight (Figures 1C and 1D). We then examined the skeletal muscle mRNA levels of several genes involved in fatty acid oxidation and very-low density lipoprotein (VLDL) uptake, which are upregulated by PPARβ/δ activation (Vázquez-Carrera 2016; Tan et al., 2016). The increased expression of *Acox*, *Acadm*, and *Vldlr* caused by GW501516 was abolished by the neutralization of GDF15 (Figure 1E), implying that this PPARβ/δ-dependent increased expression was mediated by enhanced GDF15 levels. By contrast, the increased *Cpt1b* expression caused by PPARβ/δ activation was significantly, but not completely, attenuated by the GDF15 neutralizing antibody. Last, the increase in *Pdk4* expression caused by GW501516 was not modified by the GDF15 neutralizing antibody, suggesting that the regulation of this gene by PPARβ/δ is independent of GDF15, and additional mechanisms might be involved such as direct binding of PPARβ/δ to the multiple peroxisome proliferator response elements (PPREs) located in its promoter region (Shrivastav et al., 2013) (Figure 1E).

The cellular location of lipin 1, which regulates metabolic homeostasis, determines whether fatty acids are incorporated into triglycerides or undergo mitochondrial β-oxidation (Finck et al., 2006). In the cytoplasm, lipin 1 is a phosphatidate phosphatase enzyme that promotes triglyceride accumulation and phospholipid synthesis, whereas in the nucleus, lipin 1 acts as a transcriptional coactivator regulating the induction of PPAR-γ coactivator-1α (PGC-1α)-PPARα-target genes (Finck et al., 2006) implicated in fatty acid oxidation. Interestingly, PPARβ/δ activation in the liver promotes the PGC-1α-lipin 1-PPARα pathway (Barroso et al., 2011). The levels of PPARα and PGC-1α in skeletal muscle of the HFD-fed mice was decreased compared to standard diet-fed control mice but this reduction was blocked by GW501516 (Figure 1F). The antibody reduced GW501516-induced nuclear localization of lipin 1 and increased its cytosolic levels, consistent with GDF15 promoting lipin 1 nuclear localization.

ER stress induced by HFD is involved in the development of inflammation and insulin resistance (Salvadó et al., 2015), and PPARβ/δ activation prevents lipid-induced ER stress, inflammation, and insulin resistance in skeletal muscle (Salvadó et al., 2014). Moreover, PPARβ/δ activation prevents the interleukin 6 (IL-6)-mediated increase in the expression of suppressor of cytokine signaling 3 (SOCS3) (Serrano-Marco et al., 2012), which inhibits insulin signaling through several mechanisms, including insulin receptor substrate (IRS) degradation (Howard and Flier, 2006). In the current study, the HFD increased the expression of the ER stress markers *BiP/GRP78* and *Chop* in skeletal muscle, as well as the expression levels of the pro-inflammatory cytokine *Tnfα* and *Socs3* (Figure 2A). Consistent with the above-mentioned roles of PPARβ/δ, these changes were attenuated by GW501516, but treatment with the GDF15 neutralizing antibody reverted the beneficial effects of the PPARβ/δ agonist. In agreement with the increase in ER stress caused by the HFD, activating transcription factor 4 (ATF4) protein levels and the phosphorylated levels of eukaryotic translation initiation factor 2α (eIF2α) were increased; these effects were blocked by GW501516 (Figure 2B). However, this protective role of GW501516 was abrogated when the HFD-fed mice were co-treated with the GDF15 neutralizing antibody. HFD-fed mice treated with GW501516 and IgG also exhibited an increase in the protein levels of IκBα that inhibits the pro-inflammatory transcription factor NF-κB. Accordingly, GW501516 treatment of HFD-fed mice inhibited the increase in the nuclear protein levels of the p65 subunit of NF-κB, and co-treatment with the GDF15 neutralizing antibody attenuated this inhibition (Figure 2B).

In the insulin signaling pathway, GW501516 treatment increased the protein levels of the β subunit of the insulin receptor (IRβ) (Figure 2C). This increase was completely suppressed

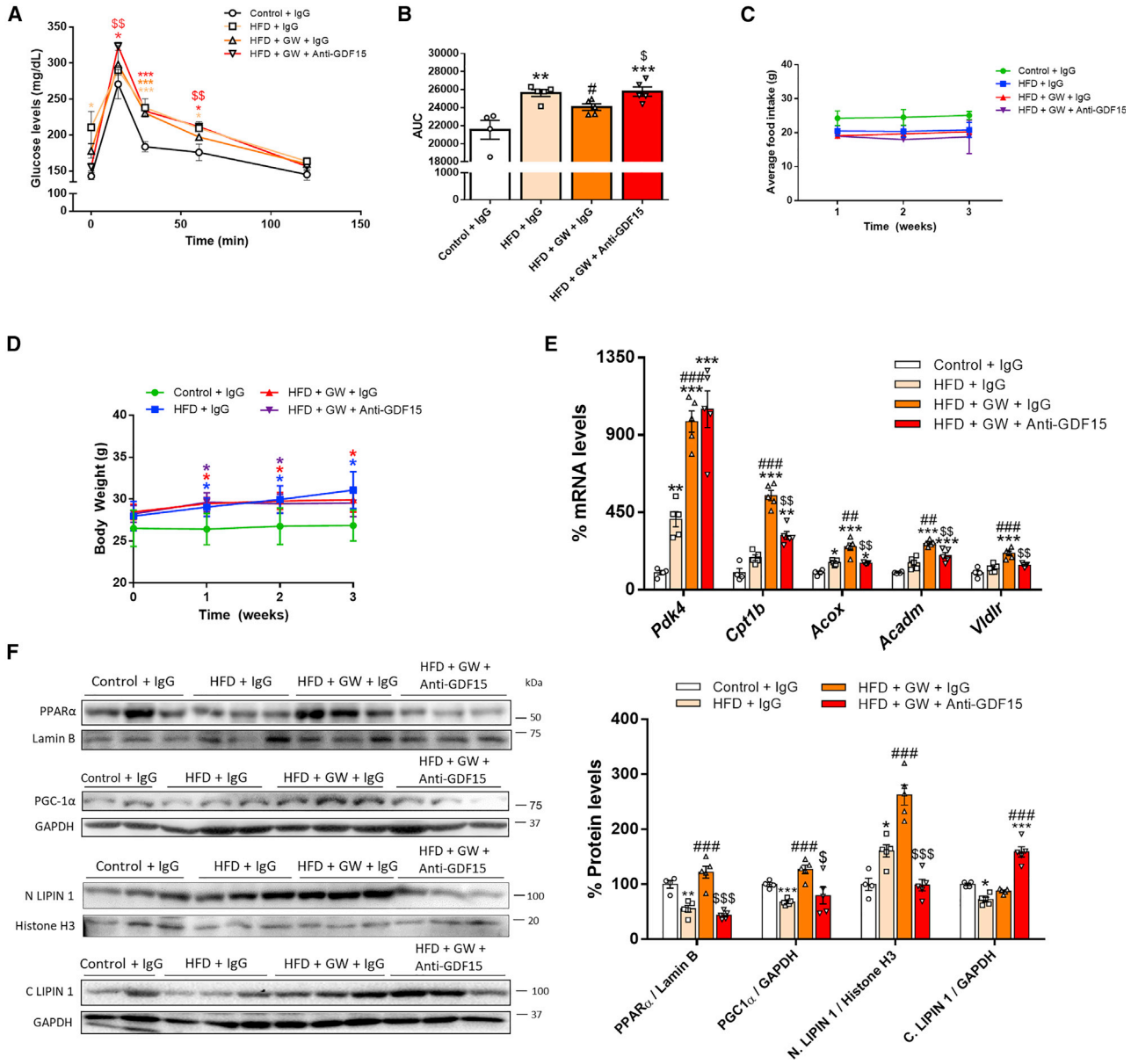

Figure 1. Neutralization of GDF15 reverts the metabolic effects of PPARβ/δ activation

(A and B) Glucose tolerance test (A) and area under the curve (AUC) (B) of mice fed standard chow (control), a HFD or a HFD plus GW501516 (GW) for 3 weeks. Three days before the end of the 3-week treatment, mice were injected once intraperitoneally with either IgG or a neutralizing antibody against GDF15.

(C) Food intake.

(D) Body weight.

(E) mRNA levels of *Pdk4*, *Cpt1b*, *Acox*, *Acadm*, and *Vldlr* in skeletal muscle.

(F) Skeletal muscle cell lysate extracts were assayed via western blot analysis with antibodies against PPARα, PGC-1α, and nuclear (N) and cytosolic (C) lipin-1.

Data are presented as the mean ± SEM (for all the experiments n = 5 animals; except for control mice where n = 4) $^{*}p < 0.05$, $^{**}p < 0.01$, and $^{***}p < 0.001$ versus control + IgG. $^{\#}p < 0.05$, $^{\#\#}p < 0.01$, and $^{\#\#\#}p < 0.001$ versus HFD + IgG group. $^{\$}p < 0.05$, $^{\$\$}p < 0.01$, and $^{\$\$\$}p < 0.001$ versus GW501516-treated mice injected with IgG. p values determined by one-way ANOVA with Tukey's post hoc test.

Source data are provided as a Source data file.

by the GDF15 neutralizing antibody. Insulin signaling can be attenuated by activation of the pro-inflammatory kinase IκB kinase β (IKK-β), which belongs to the NF-κB pathway, through phosphorylation of IRS-1 at serine residues. In agreement with the activation of the NF-κB pathway by the HFD, IRS-1 phosphorylation at Ser^{307} was increased (Figure 2C). GW501516 blocked this increase, but this protective effect was abolished by the GDF15 neutralizing antibody.

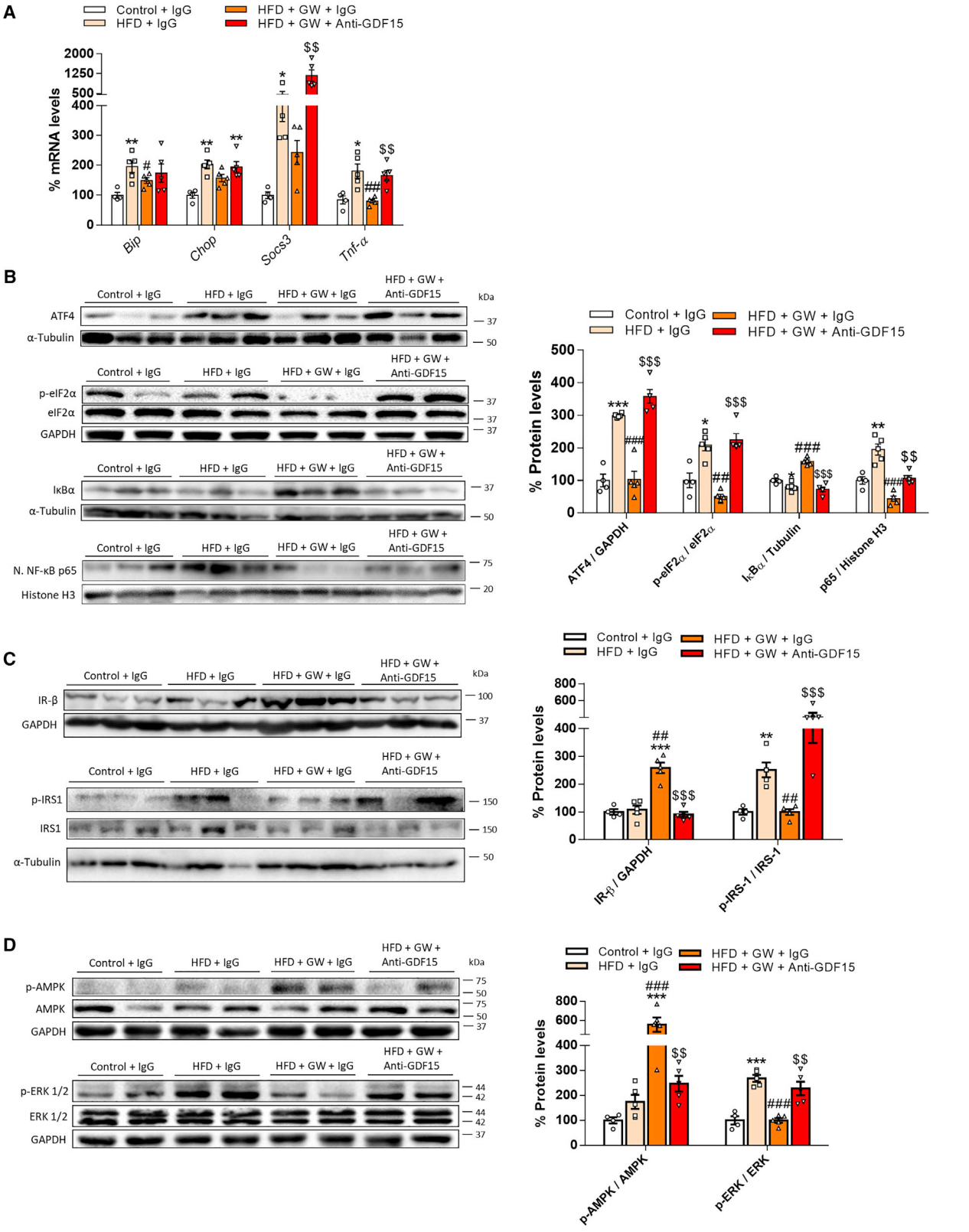

(legend on next page)

Consistent with a previous report (Salvadó et al., 2014), PPARβ/δ activation increased phospho-AMPK levels and reduced the HFD-mediated increase in the levels of phospho-ERK1/2, which is involved in a negative crosstalk with AMPK (Du et al., 2008; Hwang et al., 2013) (Figure 2D). However, these changes were not observed in mice treated with the GDF15 neutralizing antibody. Taken together, the data presented above indicate that many of the beneficial effects of pharmacological PPARβ/δ activation in muscle, including lipid metabolism, ER stress, inflammation, and insulin signaling, are attenuated or abolished by the GDF15 neutralizing antibody.

In the liver, GDF15 neutralization attenuates the beneficial effects of PPARβ/δ activation on lipid metabolism, ER stress, and the insulin signaling pathway

Mice treated with GW501516 for 6 days also showed increased *Gdf15* expression and protein levels in the liver (Figures 3A and 3B). Furthermore, the expression of the genes involved in fatty acid oxidation (*Pdk4*, *Cpt1a*, *Acadm*, and *Acox*) and of the hormone *Fgf21* was slightly increased by the HFD, with GW501516 treatment exacerbating this increase (Figure 3C). GDF15 neutralization did not reduce *Pdk4* as in skeletal muscle. Similarly, GDF15 neutralization did not significantly reduce *Cpt1a* expression, suggesting that, in contrast to its moderate effect in skeletal muscle, the increase in *Cpt1a* mRNA levels caused by GW501516 is not affected by GDF15 in the liver. However, the increased expression of *Acadm* and *Acox* caused by GW501516 was reduced by GDF15 neutralization. By contrast, the induction of the stress-response hormone *Fgf21* caused by GW501516 was strongly increased by GDF15 neutralization. Consistent with the GW501516-mediated increase in the expression of genes involved in fatty acid oxidation, the levels of serum β-hydroxybutyrate, a product of ketogenesis used as a marker of hepatic fatty acid oxidation, were significantly elevated in HFD-fed mice receiving GW501516 (Figure 3D). This was abolished by the neutralizing antibody against GDF15. The HFD increased the hepatic expression of the ER stress markers *BiP/GRP78* and *Chop* (Figure 3E). GW501516 partly protected against this increase, but this effect was lost in mice injected with the GDF15 neutralizing antibody. The same trend was observed for hepatic *Socs3* mRNA levels. In agreement with a previous study (Barroso et al., 2011), PPARβ/δ activation increased phospho-AMPK levels and decreased phospho-ERK1/2 levels (Figure 3F), which is consistent with the negative crosstalk between these kinases (Du et al., 2008; Hwang et al., 2013). When we explored the levels of signal transducer and activator of transcription 3 (STAT3), the transcription factor that regulates *Socs3* expression, we observed that the HFD increased the phosphorylated levels of STAT3 at both Tyr^{705} and Ser^{727} residues (Figure 3G). This was accompanied by increased SOCS3 protein levels. Interestingly, GW501516 prevented these increases, whereas in HFD-fed mice treated with GW501516 and the GDF15 neutralizing antibody, the protective effect of the PPARβ/δ agonist was attenuated. In line with the increased SOCS3 levels in the liver of HFD-fed mice, there was a slight decrease in IRS-1 and a marked reduction in IRS-2 protein levels (Figure 3G). These changes were blocked by GW501516, but this inhibition was lifted by the GDF15 neutralizing antibody. Collectively, these data indicate that many of the effects attained by PPARβ/δ activation in the liver depend on GDF15.

Gdf15 knockout mice present an attenuated response to PPARβ/δ activation

To clearly demonstrate that the effects resulting from pharmacological PPARβ/δ activation were dependent on GDF15, we took advantage of the *Gdf15* knockout ($Gdf15^{-/-}$) mouse model. Feeding wild-type (WT) mice with the HFD caused glucose intolerance that was ameliorated by the PPARβ/δ agonist (Figure 4A). On the contrary, this beneficial effect of GW501516 was not observed in $Gdf15^{-/-}$ mice, but in contrast an increase in glucose intolerance was detected (Figure 4A). GW501516 treatment did not significantly affect the increase in body weight caused by the HFD in WT and $Gdf15^{-/-}$ mice (Figure S3A). As expected, GW501516 reduced serum triglyceride levels (−20%) in WT mice but this effect was significantly attenuated (−12%) in $Gdf15^{-/-}$ mice (Figure 4B).

In skeletal muscle, administration of the PPARβ/δ agonist increased *Pdk4* in both WT and $Gdf15^{-/-}$ mice (Figure 4C). *Cpt1b* and *Acox* expression was also upregulated by GW501516 in WT mice but this effect was not observed in $Gdf15^{-/-}$ mice (Figure 4C). Similarly, PPARβ/δ activation reduced the increase in the expression of *BiP/GRP78*, *Socs3*, and *Mcp1* (also known as *Ccl2*) in HFD-fed WT mice, although without reaching statistical significance in the case of *BiP/GRP78*. In $Gdf15^{-/-}$ mice, the reduction in the expression of *BiP/GRP78* and *Mcp1* caused by pharmacological treatment was attenuated or abolished, whereas that of *Socs3* was not significantly affected (Figure 4D). Two proteins strongly induced by PPARβ/δ activation in skeletal muscle of WT mice, IκBα and IRβ, involved in reducing inflammation and maintaining insulin signaling, respectively, remained unchanged in $Gdf15^{-/-}$ mice (Figure 4E). Remarkably, phospho-AMPK levels were lower in

Figure 2. Neutralization of GDF15 reverts the beneficial effects of PPARβ/δ activation on ER stress and inflammation in skeletal muscle

(A) mRNA levels of *BiP/GRP78*, *Chop*, *Socs3*, and *Tnfα* in skeletal muscle of mice fed standard chow, a HFD, or a HFD plus GW501516 for 3 weeks. Three days before the end of the 3-week treatment, mice were injected once intraperitoneally with either IgG or a neutralizing antibody against GDF15.

(B) Skeletal muscle cell lysate extracts were assayed via western blot analysis with antibodies against ATF4, total and phospho-eIF2α, IκBα, and the p65 subunit of NF-κB.

(C) Total and phospho-IRS1 (Ser^{307}) and IRβ levels.

(D) Total and phospho-AMPK and total and phospho-ERK1/2 levels. Data are presented as the mean ± SEM (for all the experiments n = 5 animals; except for control mice where n = 4). $^{*}p < 0.05$, $^{**}p < 0.01$, and $^{***}p < 0.001$ versus control + IgG. $^{\#}p < 0.05$, $^{\#\#}p < 0.01$, and $^{\#\#\#}p < 0.001$ versus HFD + IgG group. $^{\$}p < 0.05$, $^{\$\$}p < 0.01$, and $^{\$\$\$}p < 0.001$ versus GW501516-treated mice injected with IgG. p values determined by one-way ANOVA with Tukey's post hoc test.

Source data are provided as a Source data file.

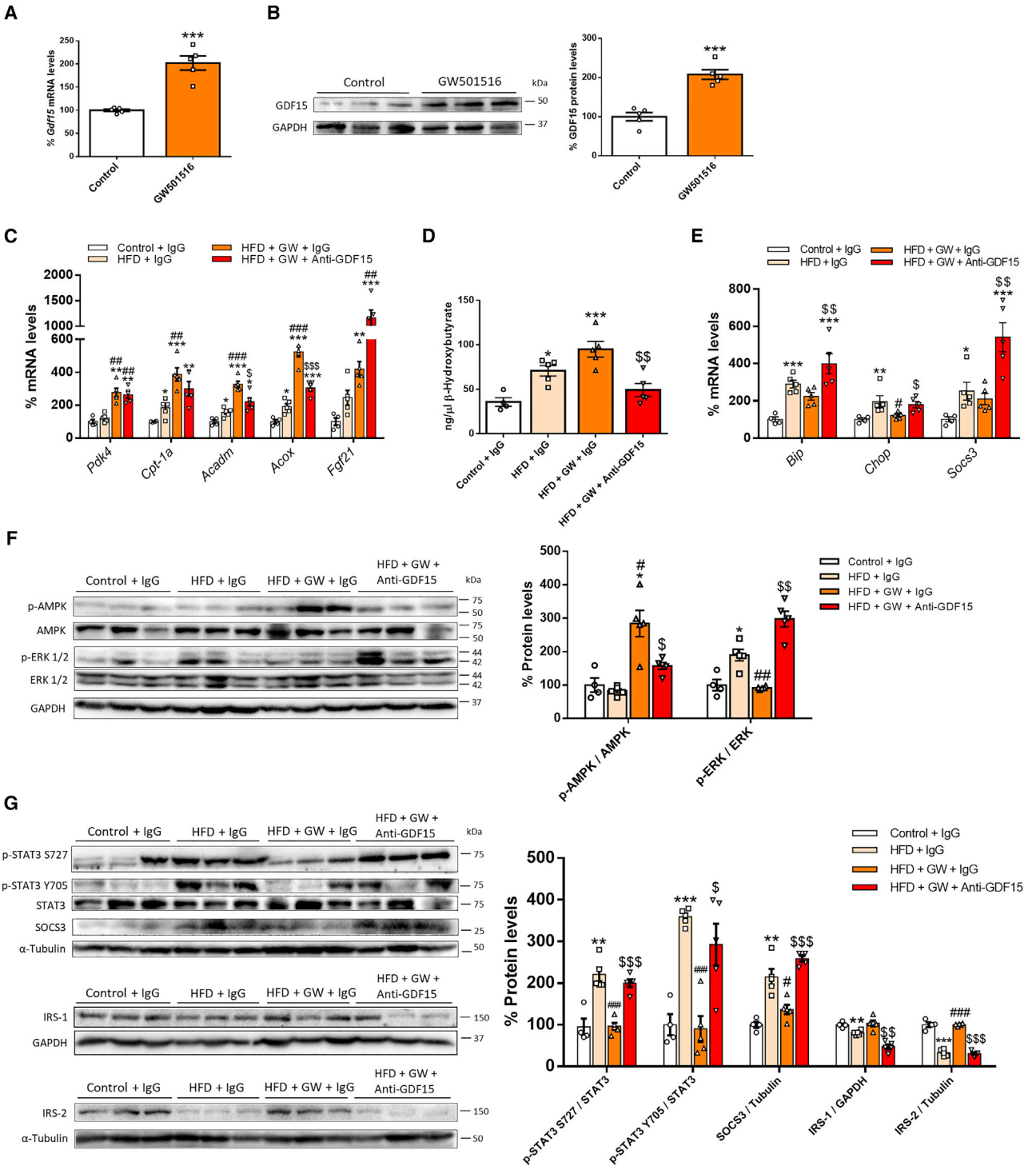

Figure 3. Neutralization of GDF15 reverts the beneficial effects of PPARβ/δ activation on ER stress and inflammation in the liver

(A and B) *Gdf15* mRNA levels (A) and GDF15 protein levels (B) in the liver of mice (n = 5 animals) treated with vehicle or 3 mg/kg/day of GW501516 for 6 days.

(C) mRNA levels of *Pdk4*, *Cpt1a*, *Acadm, Acox*, and *Fgf21* in the liver of mice (n = 5 animals; except for control mice where n = 4) fed standard chow, a HFD, or a HFD plus GW501516 for 3 weeks. Three days before the end of the 3-week treatment, mice were injected once intraperitoneally with either IgG or a neutralizing antibody against GDF15.

(D) Plasma levels of β-hydroxybutyrate.

(legend continued on next page)

skeletal muscle of *Gdf15*$^{-/-}$ mice than in WT, suggesting that GDF15 regulates phospho-AMPK levels. GW501516 restored the phosphorylated levels of this kinase in WT mice fed the HFD, but it failed to do it in *Gdf15*$^{-/-}$ mice (Figure 4E). Consistent with the negative crosstalk between AMPK and ERK1/2 (Chen et al., 2011; Hwang et al., 2013), phosphorylated levels of the latter were increased in skeletal muscle of *Gdf15*$^{-/-}$ mice compared with WT mice. Likewise, HFD feeding increased the levels of phospho-ERK1/2 and this effect was prevented by drug treatment in WT mice, but not in *Gdf15*$^{-/-}$ mice.

In the liver, H&E and oil red O (ORO) staining showed that the HFD caused a significant hepatic lipid accumulation that was slightly reduced by the PPARβ/δ agonist, although this effect did not reach statistical significance ($p = 0.06$) (Figures 5A and 5B). This modest reduction is consistent with the effect of short treatments with PPARβ/δ agonists that increase the expression of genes involved in fatty acid oxidation, but also of genes implicated in hepatic lipid deposition (Liu et al., 2011; Vázquez-Carrera 2016; Tan et al., 2016). Hepatic steatosis was remarkably higher in HFD-fed *Gdf15*$^{-/-}$ mice and it was exacerbated by GW501516. Because GDF15 mainly upregulates the expression of genes involved in fatty acid oxidation (Chung et al., 2017), the increase in hepatic steatosis and glucose intolerance caused by GW501516 in *Gdf15*$^{-/-}$ mice probably reflects that this compound does not induce the expression of genes involved in fatty acid oxidation in these mice but still promotes lipid deposition (Liu et al., 2011). Pharmacological activation of PPARβ/δ increased the expression of *Gdf15* in WT mice (Figure 5C). Moreover, consistent with the results using the neutralizing antibody against GDF15, GW501516 increased the hepatic expression of *Pdk4* in both WT and *Gdf15*$^{-/-}$ mice (Figure 5C), confirming that the regulation of this gene by PPARβ/δ is independent of GDF15. By contrast, the hepatic expression of *Cpt1a*, *Acox*, and *Fgf21* was upregulated by GW501516 in WT mice but this increase was significantly attenuated in HFD-fed *Gdf15*$^{-/-}$ mice (Figure 5C). Similarly, the increase in the expression of both *BiP*/*GRP78* and *Socs3* caused by the HFD in WT mice was significantly decreased by GW501516, whereas this reduction was attenuated in *Gdf15*$^{-/-}$ mice (Figure 5D). The same trend was observed in hepatic SOCS3 protein levels (Figure 5E). In agreement with the neutralizing antibody study, the HFD reduced the protein levels of IRS-2 in WT mice, an effect that was prevented by the PPARβ/δ agonist, whereas in *Gdf15*$^{-/-}$ mice the levels of IRS-2 were significantly lower than in WT mice, with no GW501516 effect (Figure 5E). As in skeletal muscle, GW501516 increased the hepatic levels of phospho-AMPK and reduced those of phosho-ERK1/2 in WT mice, whereas no effect was observed in *Gdf15* KO mice (Figure 5E). These data confirm that many of the beneficial effects caused by pharmacological activation of PPARβ/δ in liver, including the reduction in hepatic steatosis, depend on GDF15.

PPARβ/δ activation increases GDF15 levels through an AMPK-p53-dependent mechanism

Next, we examined the potential mechanism by which PPARβ/δ activation increases GDF15 levels. Because PPARβ/δ ligands activate AMPK (Salvadó et al., 2014), we first explored whether activation of this kinase increased GDF15 levels, which would identify a putative PPARβ/δ-AMPK-GDF15 axis. Treatment of C2C12 myotubes with the AMPK activator A769662 strongly increased the mRNA and protein levels of GDF15, which was blocked by co-incubating the cells with the AMPK inhibitor compound C (Figures S4A and S4B). Likewise, compound C blocked the increase in GDF15 and phospho-AMPK levels caused by GW501516 (Figures S4C and S4D), suggesting that the PPARβ/δ-mediated increase in GDF15 involves AMPK activation. To confirm this, C2C12 myotubes were transfected with a siRNA against both *Ampk1* and *Ampk2* to knock down both genes (Figures S4E and S4F). This significantly attenuated the increase in *Gdf15* mRNA levels caused by GW501516 (Figure S4G). AMPK is known to inhibit the p53 negative regulator, murine double minute X (MDMX). Because this repression results in the activation of p53 (Chen et al., 2011; He et al., 2014; Chen et al., 2015), a key transcription factor regulating *Gdf15* expression (Kannan et al., 2000; Li et al., 2000; Tan et al., 2000; Osada et al., 2007), we evaluated the involvement of p53 in the increased levels of GDF15 following PPARβ/δ activation. First, we examined whether under our conditions, AMPK also increased p53 levels. AMPK activation by A769662 in myotubes increased *p53* expression, which was prevented by the AMPK inhibitor compound C (Figure 6A). Interestingly, GW501516 treatment increased p53 protein levels in myotubes (Figure 6B) and the increase in p53 expression caused by GW501516 was blocked by the PPARβ/δ antagonist GSK3787 (Figure 6C) and by the knockdown of *Ampk1* and *Ampk2* (Figure 6D). Similar to these myotubes studies, mice treated with GW501516 showed increased p53 protein levels in both the skeletal muscle (Figure 6E) and liver (Figure 6F). When we treated myotubes with GW501516, we observed an increase in the protein levels of both p53 and GDF15 that was completely blocked by the selective p53 inhibitor pifithrin-α (Komarov et al., 1999) (Figure 6G). Similarly, treatment of mice with GW501516 increased both the mRNA and protein levels of p53 and GDF15 in skeletal muscle and this effect was blocked by pifithrin-α (Figures 6H and 6I). Finally, knockdown of p53 in myotubes completely inhibited the increase in GDF15 caused by GW501516 (Figure 6J). Collectively, these findings indicate that PPARβ/δ activation increases GDF15 levels through activation of the AMPK-p53 pathway.

(E) mRNA levels of *BiP*, *Chop*, and *Socs3* in the liver (n = 5 animals; except for control mice where n = 4).
(F) Liver cell lysate extracts (n = 5 animals; except for control mice where n = 4) were assayed via western blot analysis with antibodies against total and phospho-AMPK and total and phospho-ERK1/2.
(G) Total and phospho-STAT3 (Ser^{727} and Tyr^{705}), SOCS3, total IRS-1, and IRS-2 levels (n = 5 animals; except for control mice where n = 4). Data are presented as the mean ± SEM. *$p < 0.05$, **$p < 0.01$, and ***$p < 0.001$ versus control + IgG. $^{\#}p < 0.05$, $^{\#\#}p < 0.01$, and $^{\#\#\#}p < 0.001$ versus HFD + IgG group. $^{\$}p < 0.05$, $^{\$\$}p < 0.01$, and $^{\$\$\$}p < 0.001$ versus GW501516-treated mice injected with IgG. p values determined by one-way ANOVA with Tukey's post hoc test (C–G) and two-tailed unpaired Student's t test (A and B).
Source data are provided as a Source data file.

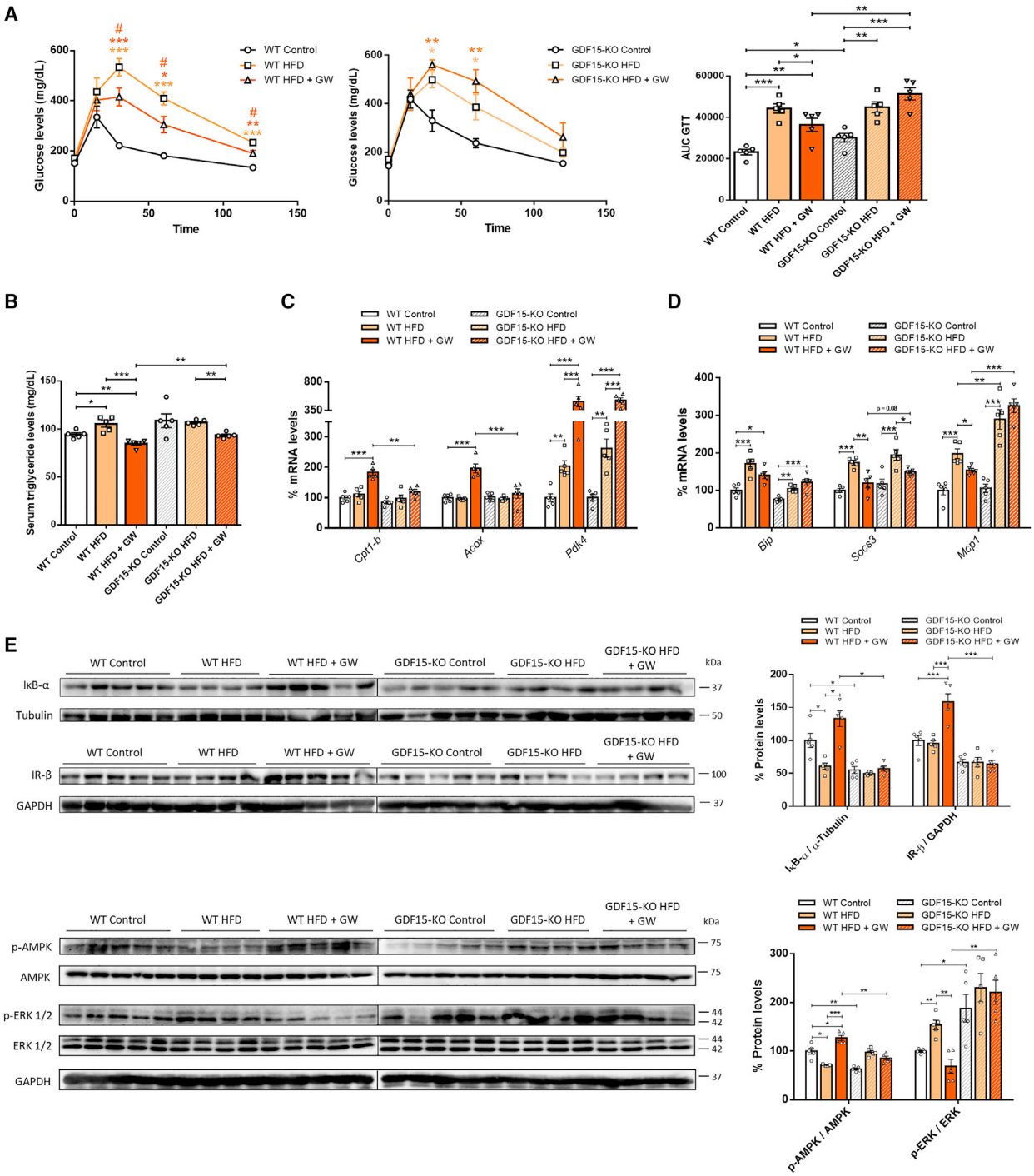

Figure 4. The beneficial effects of PPARβ/δ activation are attenuated in *Gdf15*$^{-/-}$ mice

(A) Glucose tolerance test and area under the curve (AUC) of wild-type (WT) littermates and *Gdf15*$^{-/-}$ mice (n = 5 animals) fed standard chow, an HFD or an HFD plus GW501516 for 3 weeks.

(B) Serum triglyceride levels (n = 5 animals).

(C) mRNA levels of *Cpt1b*, *Acox*, and *Pdk4* in skeletal muscle (n = 5 animals).

(D) mRNA levels of *BiP/GRP78*, *Socs3*, and *Mcp1* in skeletal muscle (n = 5 animals).

(E) Skeletal muscle cell lysate extracts were assayed via western blot analysis with antibodies against IκBα, IRβ, total and phospho-AMPK, and total and phospho-ERK1/2 levels (n = 5 animals). Data are presented as the mean ± SEM. *p < 0.05, **p < 0.01, and ***p < 0.001 versus WT or GDF15-KO control mice. #p < 0.05 versus WT or GDF15-KO mice fed a HFD. p values determined by two-way ANOVA with Tukey's post hoc test.

Source data are provided as a Source data file.

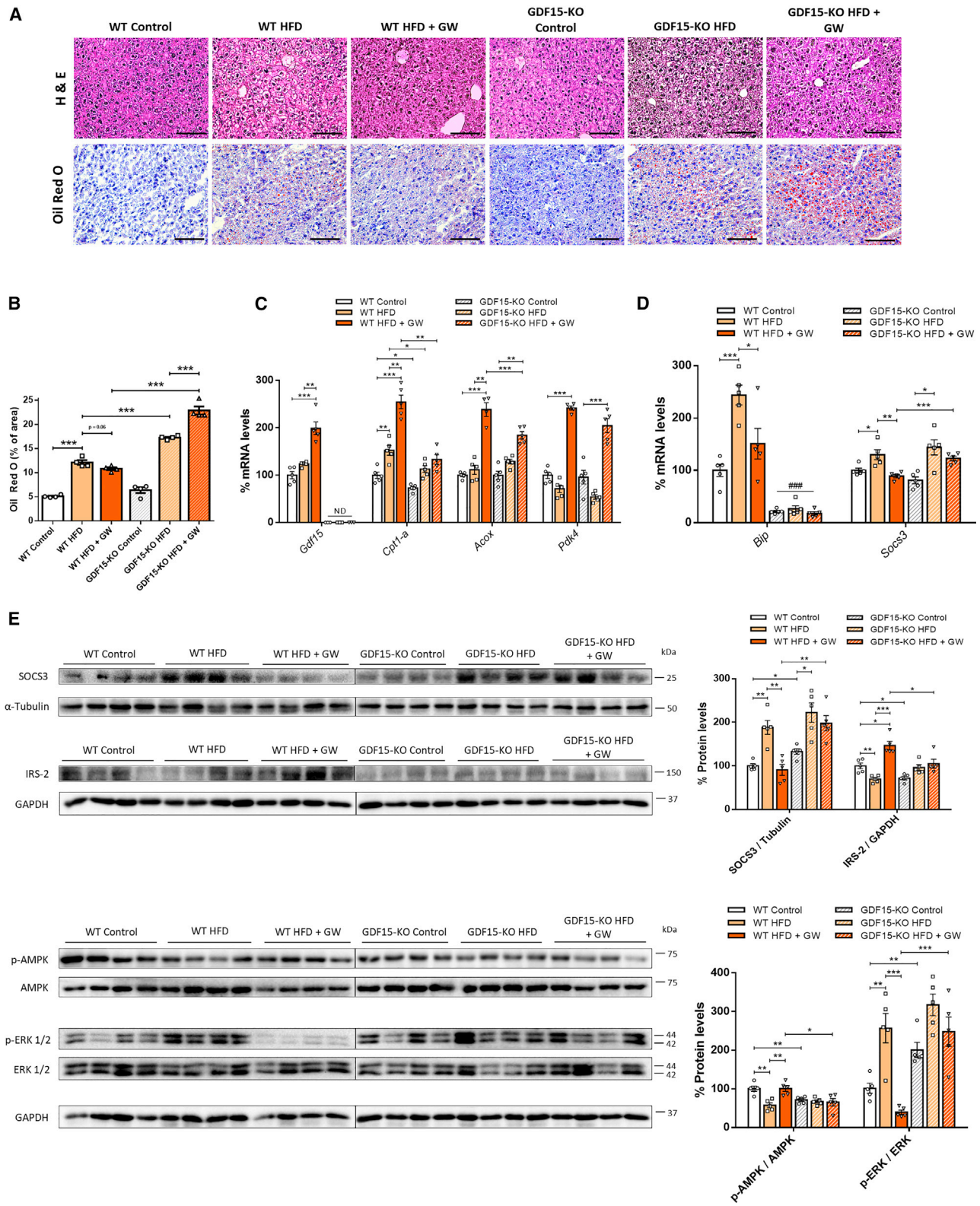

Figure 5. The beneficial effects of PPARβ/δ activation are reversed in the liver of *Gdf15*$^{-/-}$ mice

(A) H&E, oil red O (ORO) staining of livers. Scale bar, 100 μm.

(B) Quantification of ORO staining (n = 4 animals).

(legend continued on next page)

The increase in GDF15 caused by PPARβ/δ activation results in AMPK activation and does not require central effects

Because the PPARβ/δ ligand and the injection of the GDF15 neutralizing antibody did not affect food intake, we postulated that the effects caused by the PPARβ/δ-induced increase in GDF15 levels might be peripheral. To test a possible GDF15 effect independent of the brain, we exposed cultured myotubes to GW501516. We observed an increased expression of *Gdf15* and, more importantly, of three genes involved in fatty acid oxidation, *Cpt-1b*, *Acadm*, and *Acox* (Figure 7A). The stimulation of these genes caused by GW501516 was abolished when *Gdf15* was knocked down (Figures 7A and S5A). These results suggest that the increased expression of these genes is mediated by GDF15, without implicating the central receptor GFRAL, as previously reported (Chung et al., 2017). Similar results were obtained in the presence of the saturated fatty acid palmitate (Figures S5B–S5D).

Because activation of AMPK plays a pivotal role in the effects of PPARβ/δ agonists (Vázquez-Carrera, 2016), and our findings show that the GDF15 neutralization and *Gdf15* deficiency prevents the increase in phospho-AMPK levels caused by PPARβ/δ activation (Figures 2D, 3F, 4E, and 5E), together with the reduction in phospho-AMPK in skeletal muscle of *Gdf15*$^{-/-}$ mice compared with WT mice (Figure 4E), we examined whether the increased GDF15 levels caused by PPARβ/δ activation affected AMPK. Interestingly, the GW501516-mediated increase in phospho-AMPK levels in the myotubes was inhibited by the knockdown of *Gdf15*, with an opposite trend observed for ERK1/2 phosphorylation (Figure 7B), which agrees with the negative cross-talk between AMPK and ERK1/2 (Du et al., 2008; Hwang et al., 2013). These results indicate that the activation of AMPK by PPARβ/δ ligands requires increased GDF15 levels. To check this, we treated myotubes with human and mouse recombinant GDF15 and observed that this cytokine significantly increased phospho-AMPK levels, and reduced phospho-ERK1/2 levels (Figure 7C). Because some of the effects of recombinant GDF15 in cultured cells seem to involve activin receptor-like kinase (ALK) receptors 4/5/7 (ALK4/5/7) (Chung et al., 2017), we exposed cells to the ALK4/5/7 inhibitor SB431542 to examine whether these ALK isoforms were involved in the effects of GDF15 on AMPK and ERK1/2. SB431542 did not prevent the effects of either recombinant GDF15 or GW501516 on the phosphorylation status of AMPK and ERK, making unlikely the involvement of ALK4/5/7 isoforms in the observed changes (Figures S6A and S6B). Consistent with the effect observed in cultured myotubes, mice receiving a subcutaneous administration of recombinant GDF15 showed an increase in phospho-AMPK in skeletal muscle, whereas phospho-ERK1/2 was reduced (Figure 7D), confirming that GDF15 activates AMPK in skeletal muscle. To clearly confirm that the effect of GDF15 was independent of central effects, soleus muscle isolated from WT littermates and *Gdf15*$^{-/-}$ mice were incubated with GW501516 or recombinant GDF15 (Figure 7E). Both treatments increased phospho-AMPK and reduced phospho-ERK1/2 levels in WT mice but not in *Gdf15* KO mice. Based on the PPARβ/δ-induced secretion of GDF15 by myotubes and increased GDF15 serum levels in mice, we speculate that GDF15 acts via autocrine or paracrine signaling.

DISCUSSION

GDF15 is implicated in several metabolic dysfunctions, including obesity (Mullican et al., 2017) and insulin resistance (Chung et al., 2017). In fact, *Gdf15* overexpression in mice (Chrysovergis et al., 2014) and the administration of recombinant GDF15 improves glucose intolerance and increases thermogenesis and lipid metabolism (Emmerson et al., 2017; Yang et al., 2017; Mullican et al., 2017; Hsu et al., 2017). Interestingly, most of these effects are also observed when HFD-fed mice are treated with PPARβ/δ agonists (Vázquez-Carrera 2016; Tan et al., 2016). Here, we demonstrate that treatment with a PPARβ/δ agonist increases GDF15 levels through an AMPK-dependent increase in p53. *Gdf15* was previously shown to be a direct p53 target gene (Osada et al., 2007). Interestingly, the beneficial effects of pharmacological PPARβ/δ activation on glucose intolerance, fatty acid oxidation, ER stress, inflammation, and activated AMPK were abrogated by a neutralizing antibody against GDF15 and in *Gdf15*$^{-/-}$ mice, indicating that these PPARβ/δ effects were mainly mediated by GDF15. Although the improvement in glucose intolerance caused by GDF15 has been linked to a reduced food intake (Emmerson et al., 2017; Yang et al., 2017; Mullican et al., 2017; Hsu et al., 2017), we did not observe changes in either food intake or body weight, which is consistent with a previous study (Chung et al., 2017), thereby making this improvement unlikely to be the result of central effects. However, most of the effects of GDF15 reported so far are mediated centrally by GFRAL that is solely expressed in hindbrain neurons (Mullican et al., 2017). In the current study, *Gdf15* knockdown in myotubes in culture demonstrated that the increased expression of the genes involved in fatty acid oxidation caused by PPARβ/δ activation is dependent on the effects of myotube GDF15 that is secreted in the culture medium. Such effects have previously been attributed to the activation of a range of TGF-β receptors also known as the ALK receptors (ALK1-7) (Ago and Sadoshima, 2006; Johnen et al., 2007; Artz et al., 2016), which support a GDF15 autocrine signaling mechanism in the cultured myotubes. However, our findings discard the involvement of ALK4/5/7 in the regulation of AMPK by GDF15 or PPARβ/δ agonists. Further studies should elucidate the

(C) mRNA levels of *Gdf15, Pdk4*, *Cpt1b*, *Acox*, and *Fgf21* in liver of wild-type (WT) littermates and *Gdf15*$^{-/-}$ mice fed standard chow, a HFD, or a HFD plus GW501516 for 3 weeks (n = 5 animals).

(D) mRNA levels of *BiP/GRP78* and *Socs3* in liver (n = 5 animals).

(E) Liver cell lysate extracts were assayed via western blot analysis with antibodies against SOCS3, IRS-2, total and phospho-AMPK, and total and phospho-ERK1/2 (n = 5 animals). Data are presented as the mean ± SEM. ND, not detected. *p < 0.05, **p < 0.01, and ***p < 0.001. $^{###}$p < 0.001 versus indicated group. p values determined by two-way ANOVA with Tukey's post hoc test.

Source data are provided as a Source data file.

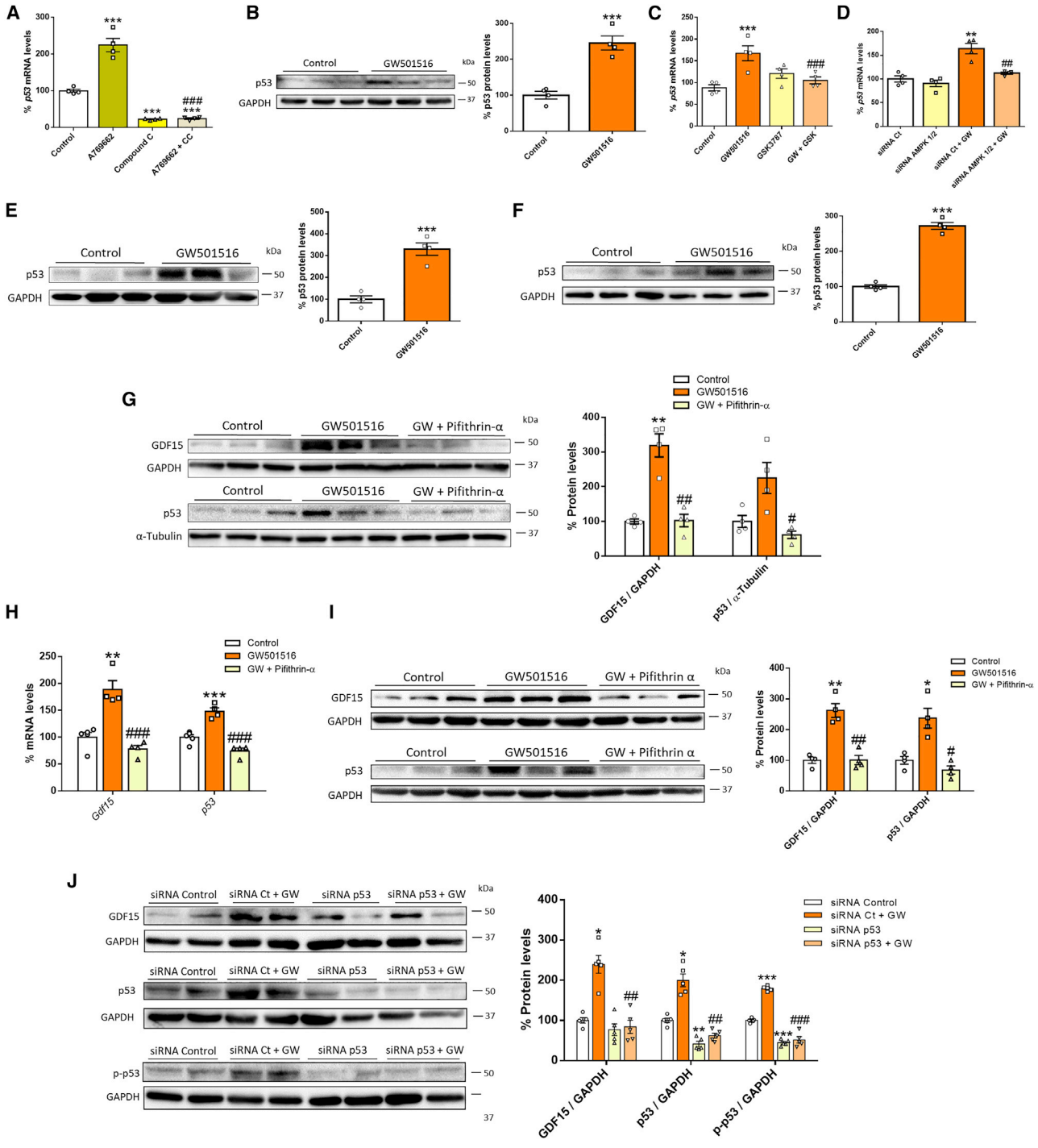

Figure 6. PPARβ/δ activation upregulates GDF15 expression through p53

(A) *p53* mRNA levels in C2C12 myotubes exposed to 60 μM of the AMPK activator A769662 for 24 h in the presence or absence of 30 μM of the AMPK inhibitor compound C (CC) (n = 4 independent cell culture experiments).

(B) p53 protein levels in C2C12 myotubes exposed to 10 μM of the PPARβ/δ agonist GW501516 (GW) for 24 h (n = 4 independent cell culture experiments).

(C and D) *p53* mRNA levels in C2C12 myotubes exposed to 10 μM of GW501516 for 24 h in the presence or absence of 10 μM of the PPARβ/δ antagonist GSK3787 (GSK) (C) or transfected with control siRNA or AMPK1/2 siRNA (D) for 48 h (n = 4 independent cell culture experiments).

(E and F) p53 protein levels in the skeletal muscle (E) and liver (F) of mice (n = 4 animals) treated with vehicle or 3 mg/kg/day of GW501516 for 6 days.

(G) GDF15 and p53 protein levels in C2C12 myotubes exposed to 10 μM of GW501516 for 24 h in the presence or absence of 10 μM of the p53 inhibitor pifithrin-α (n = 4 independent cell culture experiments).

(legend continued on next page)

mechanisms involved, including the nuclear effects of pro-GDF15 (Min et al., 2016).

The GDF15 neutralizing antibody counteracted the PPARβ/δ-dependent increased levels of the transcription factor PPARα and the transcriptional co-activators PGC-1α and lipin 1, which regulate the expression of genes involved in fatty acid oxidation, as well as in serum β-hydroxybutyrate levels. This provided evidence for GDF15 strongly contributing to the increased fatty acid oxidation caused by PPARβ/δ activation (Vázquez-Carrera, 2016). We showed that the increased expression of genes involved in fatty acid oxidation (*Cpt-1b*, *Acox*, and *Acadm*) caused by PPARβ/δ activation was blocked by the GDF15 neutralizing antibody and in *Gdf15*$^{-/-}$ mice, underscoring a critical role of this cytokine. In agreement with the regulation of the genes involved in fatty acid metabolism by GDF15, it has been previously reported that recombinant GDF15 increases the expression of *Ppara*, *Cpt1a*, and *Acadm* in skeletal muscle and the liver without changing food intake (Chung et al., 2017). As for PPARα, the hypotriglyceridemic effect caused by PPARβ/δ activation is partially mediated by the increase in the expression of genes involved in fatty acid oxidation (Vázquez-Carrera 2016; Tan et al., 2016). Here, we show that the PPARβ/δ-mediated increased expression of these genes is dependent on GDF15 and, consistently, the reduction in triglyceride levels induced by GW501516 in WT mice was attenuated in *Gdf15*$^{-/-}$ mice.

Furthermore, we found that the GDF15-mediated PPARβ/δ-dependent regulation of the genes involved in fatty acid oxidation is modulated by the activity of AMPK, an energy sensor that functions as a signaling hub, coordinating anabolic and catabolic pathways to balance nutrient supply with energy demand. Indeed, activation of this kinase plays a pivotal role in the effects of PPARβ/δ agonists (Vázquez-Carrera 2016; Tan et al., 2016). We have also previously reported that the activation of the PGC-1α-lipin 1-PPARα pathway by PPARβ/δ is associated with AMPK activation (Barroso et al., 2011). Consistent with previous studies (Salvadó et al., 2014; Barroso et al., 2011), we show here that pharmacological activation of PPARβ/δ increased the phosphorylated levels and thereby the activity of AMPK in skeletal muscle and the liver, which was abolished by the neutralizing antibody against GDF15 and in *Gdf15*$^{-/-}$ mice. Moreover, and in line with the reported inhibitory cross talk between AMPK and ERK1/2 (Du et al., 2008; Hwang et al., 2013), the increased phospho-AMPK levels caused by PPARβ/δ activation was associated to reduced phospho-ERK1/2 levels, an effect abrogated by the GDF15 neutralizing antibody and in *Gdf15*$^{-/-}$ mice. This suggests that the increase in phospho-AMPK levels and reduction in phosho-ERK1/2 levels caused by PPARβ/δ activation are dependent on increased GDF15 levels.

Lipid-induced ER stress contributes to the development of inflammation, insulin resistance and type 2 diabetes mellitus (Salvadó et al., 2015). Our findings show that feeding mice an HFD increases the expression of the markers of ER stress and inflammation, with PPARβ/δ activation attenuating these increases. However, the GDF15 neutralizing antibody or the deficiency of this hormone suppresses the PPARβ/δ protective effects. The beneficial effect of PPARβ/δ activation on ER stress and inflammation has been attributed to the activation of AMPK and the reduction of phospho-ERK1/2 levels (Coll et al., 2010; Salvadó et al., 2014). In fact, ER stress increases ERK1/2 phosphorylation in myotubes (Salvadó et al., 2014; Hwang et al., 2013), whereas ERK1/2 inhibition restores AMPK activity and insulin signaling (Hwang et al., 2013). Our findings suggest that these beneficial effects of PPARβ/δ activation on ER stress, inflammation, and insulin resistance are dependent on GDF15.

Several cytokines and hormones associated with insulin resistance induce the production of SOCS proteins, which inhibit insulin signaling (Howard and Flier, 2006). SOCS3 expression is under the transcriptional control of STAT3, which is activated by phosphorylation. Phosphorylation of STAT3 at Tyr^{705} is dependent on Janus tyrosine kinases that are activated by cytokines. In addition to Tyr^{705} phosphorylation, STAT3 also requires phosphorylation at Ser^{727} to achieve maximal transcriptional activity. Several kinases can phosphorylate STAT3 at Ser^{727}, including ERK1/2 (Decker and Kovarik, 2000). We have previously reported that pharmacological PPARβ/δ activation suppresses IL-6-induced STAT3 activation by inhibiting ERK1/2 phosphorylation and preventing the reduction in phospho-AMPK levels (Serrano-Marco et al., 2012). The findings of the current study demonstrate that the effect of PPARβ/δ on STAT3 phosphorylation and SOCS3 and IRS levels also depends on increased GDF15 levels.

In this study, we report that GDF15 activates AMPK. In support of this mechanism, our findings show that the increase in phospho-AMPK caused by pharmacological activation of PPARβ/δ is suppressed in skeletal muscle and the liver of mice treated with a neutralizing antibody against GDF15 and in *Gdf15*$^{-/-}$ mice. In addition, treatment with GDF15 increases phospho-AMPK *in vivo* and in cell culture and isolated skeletal muscle, the latter suggesting that this effect is independent of central effects. Finally, *Gdf15*$^{-/-}$ mice show reduced levels of phospho-AMPK in skeletal muscle compared with WT mice. AMPK activation by GDF15 would result in reduced ERK1/2 phosphorylation, in line with previous studies reporting that GDF15 decreases phospho-ERK1/2 levels (Subramaniam et al., 2003; Xu et al., 2014). Based on our results, we propose that the enhanced GDF15 levels caused by PPARβ/δ activation prolong the increase in phospho-AMPK levels and the reduction in phospho-ERK1/2 levels. Therefore, we can postulate the following scenario (Figure 7F), although we cannot discard the involvement of alternative pathways. First, and as

(H and I) *Gdf15* and *p53* mRNA levels (H) and GDF15 and p53 protein levels (I) in the skeletal muscle of mice (n = 4 animals) treated with either vehicle plus GW501516 for 6 days or GW501516 plus pifithrin-α.

(J) GDF15, phospho-p53, and p53 levels in C2C12 myotubes exposed to 10 μM of GW501516 for 24 h and transfected with control siRNA or p53 siRNA for 48 h (n = 4 independent cell culture experiments). Data are presented as the mean ± SEM. *p < 0.05, **p < 0.01, and ***p < 0.001 versus control. $^{\#}$p < 0.05, $^{\#\#}$p < 0.01, and $^{\#\#\#}$p < 0.001 versus A769662- or GW501516-treated cells or animals. p values determined by one-way ANOVA with Tukey's post hoc test (A–D and G–J) and two-tailed unpaired Student's t test (E and F).

Source data are provided as a Source data file.

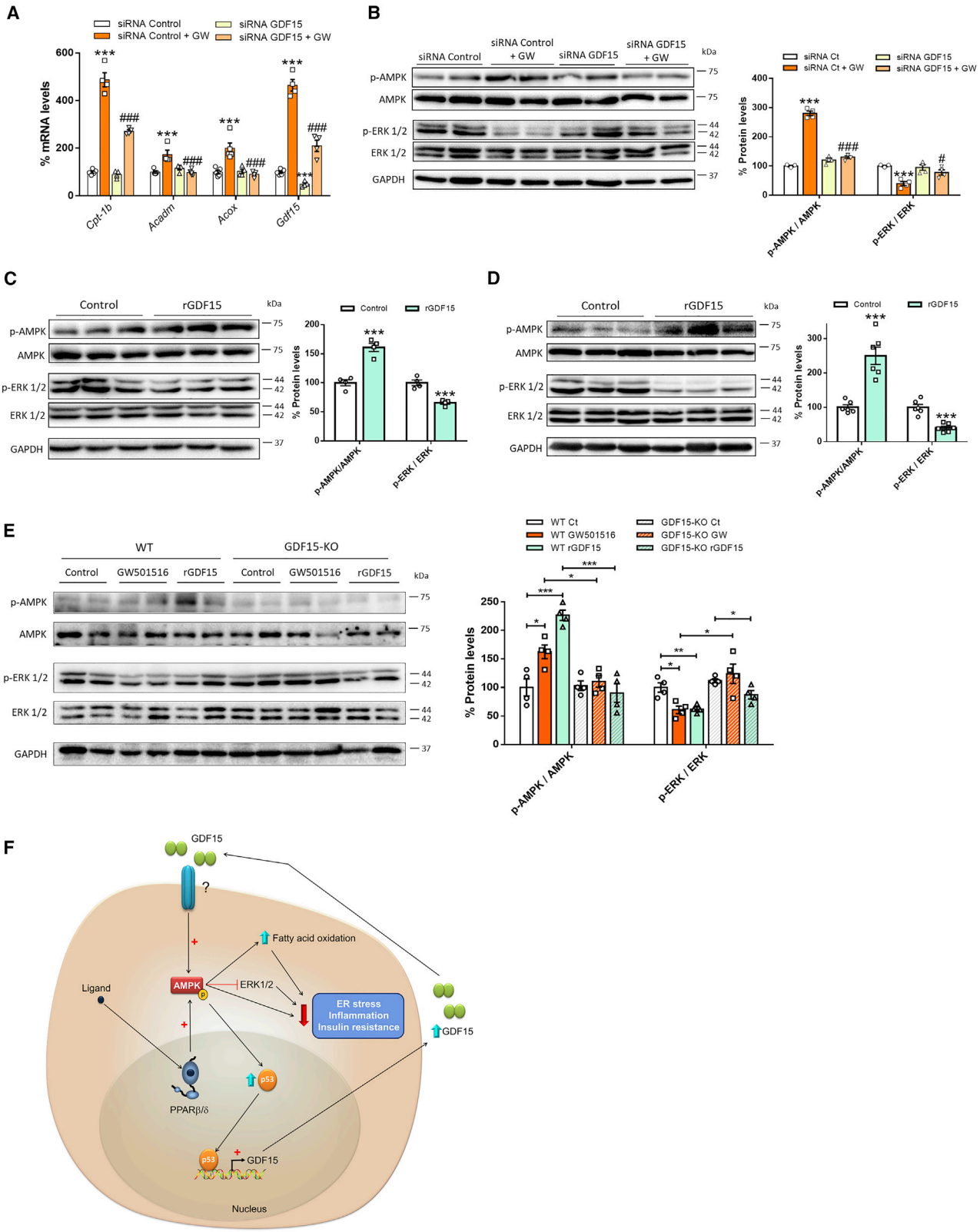

(legend on next page)

previously reported, PPARβ/δ activation leads to AMPK activation by changes in the AMP levels (Salvadó et al., 2014) or through the increased expression of calcium calmodulin-dependent protein kinase kinase β (CaMKKβ) (Koh et al., 2017). This activation leads to several effects, including enhanced p53 levels that increase GDF15 expression and circulating levels. The increase in GDF15 levels then sustains AMPK activation and the subsequent reduction in phospho-ERK1/2 levels, thus perpetuating the activation of AMPK, which reduces ER stress, inflammation, and insulin resistance.

Overall, the findings of this study highlight a regulatory mechanism by which the activation of the AMPK-p53 pathway by PPARβ/δ ligands results in increased levels of GDF15, which in turn mediates the metabolic effects of these ligands by prolonging AMPK activation. Because activation of the PPARβ/δ-AMPK pathway in skeletal muscle enhances physical performance (Narkar et al., 2008; Koh et al., 2017) and ameliorates inflammation and insulin resistance (Vázquez-Carrera 2016; Tan et al., 2016), the findings of this work indicate that GDF15 may become a pharmacological target to potentiate this pathway.

Limitations of the study

Challenges in exploring the receptors mediating the peripheral effects of GDF15

The findings of this study point to an effect of GDF15 on AMPK that is independent of central GFRAL and is not the result of changes in food intake. In fact, the increased GDF15 plasma levels (~150 pg/mL) provoked by the PPARβ/δ ligand were lower than the plasma levels (~2,000 pg/mL) reported to reduce food intake, corresponding to a GDF15 dose of 20 μg/kg, whereas a lower dose (2 μg/kg) had no effect on food intake at any of the time points studied (Borner et al., 2020). This is consistent with the reduction in food intake caused by pharmacological doses of GDF15, whereas physiological induction of endogenous circulating GDF15 levels did not affect food intake (Klein et al., 2021). However, the potential involvement of GFRAL in the PPARβ/δ-mediated increase in GDF15 still needs to be formally rejected in future studies by using GFRAL knockout mice or neutralizing antibodies against this receptor. Therefore, a limitation of this study is that we cannot totally exclude that the effects caused by PPARβ/δ ligand through the upregulation of GDF15 *in vivo* might involve GFRAL through changes in physical activity or yet-to-be-determined GDF15 physiological effects. By contrast, the *in vitro* and *ex vivo* findings of this study show that GDF15 activates AMPK in cultured C2C12 myotubes and isolated skeletal muscle, suggesting that this effect of GDF15 is the result of autocrine or paracrine effects of this cytokine, ruling out central effects. Because *Gfral* mRNA was virtually absent in C2C12 cells (Yang et al., 2017) (Figure S7) and skeletal muscle (Laurens et al., 2020) (Figure S7), the GDF15-mediated activation of AMPK in isolated skeletal muscle and cultured myotubes seems to exclude this receptor. This leads to the question of which is the new potential receptor responsible for the autocrine/paracrine effects of GDF15 in skeletal muscle. This is challenging because GFRAL was robustly identified as the receptor mediating the effects of GDF15 (Hsu et al., 2017; Mullican et al., 2017; Yang et al., 2017). However, several additional membrane-expressed proteins have been suggested to be additional GDF15-binding partners, although with lower affinity (Hsu et al., 2017; Mullican et al., 2017). Moreover, we cannot exclude the involvement of GDF15-mediated nuclear effects because it has been reported that this cytokine controls transcription (Min et al., 2016). Future studies are warranted to uncover the receptor involved in the autocrine/paracrine effects of GDF15 in skeletal muscle.

STAR★METHODS

Detailed methods are provided in the online version of this paper and include the following:

- KEY RESOURCES TABLE
- RESOURCE AVAILABILITY
  - Lead contact
  - Materials availability
  - Data and code availability
- EXPERIMENTAL MODEL AND SUBJECT DETAILS
  - Mice
  - Cell lines
- METHOD DETAILS
  - Animal treatments
  - Liver histology
  - Cell culture
  - *Ex vivo* skeletal muscle incubation
  - Reverse Transcriptase-Polymerase Chain Reaction and Quantitative Polymerase Chain Reaction
  - Western blot analysis

Figure 7. PPARβ/δ activation requires increased GDF15 expression to maintain the increase in phospho-AMPK levels

(A) *Cpt-1b*, *Acadm*, *Acox*, and *Gdf15* mRNA levels in C2C12 myotubes in the presence or absence of 10 μM of the PPARβ/δ agonist GW501516 for 24 h and transfected with control siRNA or GDF15 siRNA for 48 h (n = 4 independent cell culture experiments).

(B) Total and phospho-AMPK and total and phospho-ERK1/2 protein levels in C2C12 myotubes in the presence or absence of 10 μM of GW501516 for 24 h and transfected with control siRNA or GDF15 siRNA (n = 4 independent cell culture experiments).

(C) Total and phospho-AMPK and total and phospho-ERK1/2 protein levels in C2C12 myotubes exposed to human GDF15 (100 ng/L) for 24 h (n = 4 independent cell culture experiments).

(D) Immunoblot analysis of total and phospho-AMPK and total and phospho-ERK1/2 protein in skeletal muscle of mice (n = 6 animals) treated with GDF15 (two subcutaneous injections of 0.05 mg/kg GDF15 for 2 days).

(E) Total and phospho-AMPK and total and phospho-ERK1/2 protein levels in isolated soleus muscles from WT and *Gdf15* KO mice incubated with 10 μM GW501516 or 500 ng/mL of recombinant mouse GDF15 for 4 h (n = 4 muscles).

(F) Proposed mechanism by which PPARβ/δ regulates GDF15 levels and AMPK activation. Data are presented as the mean ± SEM. ***$p < 0.001$ versus control. ###$p < 0.001$ and #$p < 0.05$ versus siRNA control cells treated with GW501516. p values determined by one-way ANOVA with Tukey's post hoc test (A and B) and two-tailed unpaired Student's t test (C and D).

Source data are provided as a Source data file.

- QUANTIFICATION AND STATISTICAL ANALYSIS
  - Statistical analysis

SUPPLEMENTAL INFORMATION

Supplemental information can be found online at https://doi.org/10.1016/j.celrep.2021.109501.

ACKNOWLEDGMENTS

We would like to thank the University of Barcelona's Language Services for revising the manuscript. CIBER de Diabetes y Enfermedades Metabólicas Asociadas (CIBERDEM) is a Carlos III Health Institute project. CERCA Programme/Generalitat de Catalunya. This study was partly supported by grants from the Spanish Ministry of Economy and Competitiveness (SAF2015-64146-R and RTI2018-093999-B-100) and European Union ERDF funds.

AUTHOR CONTRIBUTIONS

D.A.-R., E.B., A.G., J.P.-D., L.P., M.R., and M.V.-C. conducted the experiments. D.A.-R., M.R., X.P., W.W., and M.V.-C. analyzed the data and reviewed the results. D.A.-R., A.G., and M.V.-C. designed the experiments and reviewed the results. M.V.-C. was primarily responsible for writing the manuscript. All authors contributed to manuscript editing and have approved the final version.

DECLARATION OF INTERESTS

The authors declare no competing interests.

Received: October 8, 2019
Revised: March 31, 2021
Accepted: July 15, 2021
Published: August 10, 2021

REFERENCES

Ago, T., and Sadoshima, J. (2006). GDF15, a cardioprotective TGF-beta superfamily protein. Circ. Res. *98*, 294–297.

Artz, A., Butz, S., and Vestweber, D. (2016). GDF-15 inhibits integrin activation and mouse neutrophil recruitment through the ALK-5/TGF-βRII heterodimer. Blood *128*, 529–541.

Baek, S.J., Kim, J.S., Nixon, J.B., DiAugustine, R.P., and Eling, T.E. (2004). Expression of NAG-1, a transforming growth factor-beta superfamily member, by troglitazone requires the early growth response gene EGR-1. J. Biol. Chem. *279*, 6883–6892.

Baek, S.J., Kim, J.S., Moore, S.M., Lee, S.H., Martinez, J., and Eling, T.E. (2005). Cyclooxygenase inhibitors induce the expression of the tumor suppressor gene EGR-1, which results in the up-regulation of NAG-1, an antitumorigenic protein. Mol. Pharmacol. *67*, 356–364.

Barroso, E., Rodríguez-Calvo, R., Serrano-Marco, L., Astudillo, A.M., Balsinde, J., Palomer, X., and Vázquez-Carrera, M. (2011). The PPARβ/δ activator GW501516 prevents the down-regulation of AMPK caused by a high-fat diet in liver and amplifies the PGC-1α-Lipin 1-PPARα pathway leading to increased fatty acid oxidation. Endocrinology *152*, 1848–1859.

Bojic, L.A., Telford, D.E., Fullerton, M.D., Ford, R.J., Sutherland, B.G., Edwards, J.Y., Sawyez, C.G., Gros, R., Kemp, B.E., Steinberg, G.R., and Huff, M.W. (2014). PPARδ activation attenuates hepatic steatosis in Ldlr-/- mice by enhanced fat oxidation, reduced lipogenesis, and improved insulin sensitivity. J. Lipid Res. *55*, 1254–1266.

Borner, T., Wald, H.S., Ghidewon, M.Y., Zhang, B., Wu, Z., De Jonghe, B.C., Breen, D., and Grill, H.J. (2020). GDF15 Induces an Aversive Visceral Malaise State that Drives Anorexia and Weight Loss. Cell Rep. *31*, 107543.

Chen, M.B., Wu, X.Y., Gu, J.H., Guo, Q.T., Shen, W.X., and Lu, P.H. (2011). Activation of AMP-activated protein kinase contributes to doxorubicin-induced cell death and apoptosis in cultured myocardial H9c2 cells. Cell Biochem. Biophys. *60*, 311–322.

Chen, M.B., Jiang, Q., Liu, Y.Y., Zhang, Y., He, B.S., Wei, M.X., Lu, J.W., Ji, Y., and Lu, P.H. (2015). C6 ceramide dramatically increases vincristine sensitivity both in vivo and in vitro, involving AMP-activated protein kinase-p53 signaling. Carcinogenesis *36*, 1061–1070.

Chrysovergis, K., Wang, X., Kosak, J., Lee, S.H., Kim, J.S., Foley, J.F., Travlos, G., Singh, S., Baek, S.J., and Eling, T.E. (2014). NAG-1/GDF-15 prevents obesity by increasing thermogenesis, lipolysis and oxidative metabolism. Int. J. Obes. *38*, 1555–1564.

Chung, H.K., Ryu, D., Kim, K.S., Chang, J.Y., Kim, Y.K., Yi, H.S., Kang, S.G., Choi, M.J., Lee, S.E., Jung, S.B., et al. (2017). Growth differentiation factor 15 is a myomitokine governing systemic energy homeostasis. J. Cell Biol. *216*, 149–165.

Coll, T., Alvarez-Guardia, D., Barroso, E., Gómez-Foix, A.M., Palomer, X., Laguna, J.C., and Vázquez-Carrera, M. (2010). Activation of peroxisome proliferator-activated receptor-delta by GW501516 prevents fatty acid-induced nuclear factor-kappaB activation and insulin resistance in skeletal muscle cells. Endocrinology *151*, 1560–1569.

Decker, T., and Kovarik, P. (2000). Serine phosphorylation of STATs. Oncogene *19*, 2628–2637.

Ding, Q., Mracek, T., Gonzalez-Muniesa, P., Kos, K., Wilding, J., Trayhurn, P., and Bing, C. (2009). Identification of macrophage inhibitory cytokine-1 in adipose tissue and its secretion as an adipokine by human adipocytes. Endocrinology *150*, 1688–1696.

Du, J., Guan, T., Zhang, H., Xia, Y., Liu, F., and Zhang, Y. (2008). Inhibitory crosstalk between ERK and AMPK in the growth and proliferation of cardiac fibroblasts. Biochem. Biophys. Res. Commun. *368*, 402–407.

Emmerson, P.J., Wang, F., Du, Y., Liu, Q., Pickard, R.T., Gonciarz, M.D., Coskun, T., Hamang, M.J., Sindelar, D.K., Ballman, K.K., et al. (2017). The metabolic effects of GDF15 are mediated by the orphan receptor GFRAL. Nat. Med. *23*, 1215–1219.

Fairlie, W.D., Moore, A.G., Bauskin, A.R., Russell, P.K., Zhang, H.P., and Breit, S.N. (1999). MIC-1 is a novel TGF-beta superfamily cytokine associated with macrophage activation. J. Leukoc. Biol. *65*, 2–5.

Finck, B.N., Gropler, M.C., Chen, Z., Leone, T.C., Croce, M.A., Harris, T.E., Lawrence, J.C., Jr., and Kelly, D.P. (2006). Lipin 1 is an inducible amplifier of the hepatic PGC-1alpha/PPARalpha regulatory pathway. Cell Metab. *4*, 199–210.

Gumà, A., Testar, X., Palacín, M., and Zorzano, A. (1988). Insulin-stimulated alpha-(methyl)aminoisobutyric acid uptake in skeletal muscle. Evidence for a short-term activation of uptake independent of Na+ electrochemical gradient and protein synthesis. Biochem. J. *253*, 625–629.

He, G., Zhang, Y.W., Lee, J.H., Zeng, S.X., Wang, Y.V., Luo, Z., Dong, X.C., Viollet, B., Wahl, G.M., and Lu, H. (2014). AMP-activated protein kinase induces p53 by phosphorylating MDMX and inhibiting its activity. Mol. Cell. Biol. *34*, 148–157.

Howard, J.K., and Flier, J.S. (2006). Attenuation of leptin and insulin signaling by SOCS proteins. Trends Endocrinol. Metab. *17*, 365–371.

Hromas, R., Hufford, M., Sutton, J., Xu, D., Li, Y., and Lu, L. (1997). PLAB, a novel placental bone morphogenetic protein. Biochim. Biophys. Acta *1354*, 40–44.

Hsu, J.Y., Crawley, S., Chen, M., Ayupova, D.A., Lindhout, D.A., Higbee, J., Kutach, A., Joo, W., Gao, Z., Fu, D., et al. (2017). Non-homeostatic body weight regulation through a brainstem-restricted receptor for GDF15. Nature *550*, 255–259.

Hwang, S.L., Jeong, Y.T., Li, X., Kim, Y.D., Lu, Y., Chang, Y.C., Lee, I.K., and Chang, H.W. (2013). Inhibitory cross-talk between the AMPK and ERK pathways mediates endoplasmic reticulum stress-induced insulin resistance in skeletal muscle. Br. J. Pharmacol. *169*, 69–81.

Johnen, H., Lin, S., Kuffner, T., Brown, D.A., Tsai, V.W., Bauskin, A.R., Wu, L., Pankhurst, G., Jiang, L., Junankar, S., et al. (2007). Tumor-induced anorexia

and weight loss are mediated by the TGF-beta superfamily cytokine MIC-1. Nat. Med. *13*, 1333–1340.

Johnen, H., Kuffner, T., Brown, D.A., Wu, B.J., Stocker, R., and Breit, S.N. (2012). Increased expression of the TGF-b superfamily cytokine MIC-1/GDF15 protects ApoE(–/–) mice from the development of atherosclerosis. Cardiovasc. Pathol. *21*, 499–505.

Kannan, K., Amariglio, N., Rechavi, G., and Givol, D. (2000). Profile of gene expression regulated by induced p53: connection to the TGF-beta family. FEBS Lett. *470*, 77–82.

Klein, A.B., Nicolaisen, T.S., Ørtenblad, N., Gejl, K.D., Jensen, R., Fritzen, A.M., Larsen, E.L., Karstoft, K., Poulsen, H.E., Morville, T., et al. (2021). Pharmacological but not physiological GDF15 suppresses feeding and the motivation to exercise. Nat. Commun. *12*, 1041.

Koh, J.H., Hancock, C.R., Terada, S., Higashida, K., Holloszy, J.O., and Han, D.H. (2017). PPARβ Is Essential for Maintaining Normal Levels of PGC-1α and Mitochondria and for the Increase in Muscle Mitochondria Induced by Exercise. Cell Metab. *25*, 1176–1185.e5.

Komarov, P.G., Komarova, E.A., Kondratov, R.V., Christov-Tselkov, K., Coon, J.S., Chernov, M.V., and Gudkov, A.V. (1999). A chemical inhibitor of p53 that protects mice from the side effects of cancer therapy. Science *285*, 1733–1737.

Laurens, C., Parmar, A., Murphy, E., Carper, D., Lair, B., Maes, P., Vion, J., Boulet, N., Fontaine, C., Marquès, M., et al. (2020). Growth and differentiation factor 15 is secreted by skeletal muscle during exercise and promotes lipolysis in humans. JCI Insight *5*, e131870.

Lee, C.H., Olson, P., Hevener, A., Mehl, I., Chong, L.W., Olefsky, J.M., Gonzalez, F.J., Ham, J., Kang, H., Peters, J.M., and Evans, R.M. (2006). PPARdelta regulates glucose metabolism and insulin sensitivity. Proc. Natl. Acad. Sci. USA *103*, 3444–3449.

Li, P.X., Wong, J., Ayed, A., Ngo, D., Brade, A.M., Arrowsmith, C., Austin, R.C., and Klamut, H.J. (2000). Placental transforming growth factor-beta is a downstream mediator of the growth arrest and apoptotic response of tumor cells to DNA damage and p53 overexpression. J. Biol. Chem. *275*, 20127–20135.

Liu, S., Hatano, B., Zhao, M., Yen, C.C., Kang, K., Reilly, S.M., Gangl, M.R., Gorgun, C., Balschi, J.A., Ntambi, J.M., and Lee, C.H. (2011). Role of peroxisome proliferator-activated receptor δ/β in hepatic metabolic regulation. J. Biol. Chem. *286*, 1237–1247.

Macia, L., Tsai, V.W., Nguyen, A.D., Johnen, H., Kuffner, T., Shi, Y.C., Lin, S., Herzog, H., Brown, D.A., Breit, S.N., and Sainsbury, A. (2012). Macrophage inhibitory cytokine 1 (MIC-1/GDF15) decreases food intake, body weight and improves glucose tolerance in mice on normal & obesogenic diets. PLoS ONE *7*, e34868.

McGrath, J.C., and Lilley, E. (2015). Implementing guidelines on reporting research using animals (ARRIVE etc.): new requirements for publication in BJP. Br. J. Pharmacol. *172*, 3189–3193.

Min, K.W., Liggett, J.L., Silva, G., Wu, W.W., Wang, R., Shen, R.F., Eling, T.E., and Baek, S.J. (2016). NAG-1/GDF15 accumulates in the nucleus and modulates transcriptional regulation of the Smad pathway. Oncogene *35*, 377–388.

Mullican, S.E., Lin-Schmidt, X., Chin, C.N., Chavez, J.A., Furman, J.L., Armstrong, A.A., Beck, S.C., South, V.J., Dinh, T.Q., Cash-Mason, T.D., et al. (2017). GFRAL is the receptor for GDF15 and the ligand promotes weight loss in mice and nonhuman primates. Nat. Med. *23*, 1150–1157.

Narkar, V.A., Downes, M., Yu, R.T., Embler, E., Wang, Y.X., Banayo, E., Mihaylova, M.M., Nelson, M.C., Zou, Y., Juguilon, H., et al. (2008). AMPK and PPARdelta agonists are exercise mimetics. Cell *134*, 405–415.

Osada, M., Park, H.L., Park, M.J., Liu, J.W., Wu, G., Trink, B., and Sidransky, D. (2007). A p53-type response element in the GDF15 promoter confers high specificity for p53 activation. Biochem. Biophys. Res. Commun. *354*, 913–918.

Paralkar, V.M., Vail, A.L., Grasser, W.A., Brown, T.A., Xu, H., Vukicevic, S., Ke, H.Z., Qi, H., Owen, T.A., and Thompson, D.D. (1998). Cloning and characterization of a novel member of the transforming growth factor-beta/bone morphogenetic protein family. J. Biol. Chem. *273*, 13760–13767.

Salvadó, L., Barroso, E., Gómez-Foix, A.M., Palomer, X., Michalik, L., Wahli, W., and Vázquez-Carrera, M. (2014). PPARβ/δ prevents endoplasmic reticulum stress-associated inflammation and insulin resistance in skeletal muscle cells through an AMPK-dependent mechanism. Diabetologia *57*, 2126–2135.

Salvadó, L., Palomer, X., Barroso, E., and Vázquez-Carrera, M. (2015). Targeting endoplasmic reticulum stress in insulin resistance. Trends Endocrinol. Metab. *26*, 438–448.

Sasahara, A., Tominaga, K., Nishimura, T., Yano, M., Kiyokawa, E., Noguchi, M., Noguchi, M., Kanauchi, H., Ogawa, T., Minato, H., et al. (2017). An autocrine/paracrine circuit of growth differentiation factor (GDF) 15 has a role for maintenance of breast cancer stem-like cells. Oncotarget *8*, 24869–24881.

Serrano-Marco, L., Barroso, E., El Kochairi, I., Palomer, X., Michalik, L., Wahli, W., and Vázquez-Carrera, M. (2012). The peroxisome proliferator-activated receptor (PPAR) β/δ agonist GW501516 inhibits IL-6-induced signal transducer and activator of transcription 3 (STAT3) activation and insulin resistance in human liver cells. Diabetologia *55*, 743–751.

Shrivastav, S., Zhang, L., Okamoto, K., Lee, H., Lagranha, C., Abe, Y., Balasubramanyam, A., Lopaschuk, G.D., Kino, T., and Kopp, J.B. (2013). HIV-1 Vpr enhances PPARβ/δ-mediated transcription, increases PDK4 expression, and reduces PDC activity. Mol. Endocrinol. *27*, 1564–1576.

Subramaniam, S., Strelau, J., and Unsicker, K. (2003). Growth differentiation factor-15 prevents low potassium-induced cell death of cerebellar granule neurons by differential regulation of Akt and ERK pathways. J. Biol. Chem. *278*, 8904–8912.

Tan, M., Wang, Y., Guan, K., and Sun, Y. (2000). PTGF-beta, a type beta transforming growth factor (TGF-beta) superfamily member, is a p53 target gene that inhibits tumor cell growth via TGF-beta signaling pathway. Proc. Natl. Acad. Sci. USA *97*, 109–114.

Tan, N.S., Vázquez-Carrera, M., Montagner, A., Sng, M.K., Guillou, H., and Wahli, W. (2016). Transcriptional control of physiological and pathological processes by the nuclear receptor PPARβ/δ. Prog. Lipid Res. *64*, 98–122.

Tsai, V.W.W., Husaini, Y., Sainsbury, A., Brown, D.A., and Breit, S.N. (2018). The MIC-1/GDF15-GFRAL Pathway in Energy Homeostasis: Implications for Obesity, Cachexia, and Other Associated Diseases. Cell Metab. *28*, 353–368.

Vázquez-Carrera, M. (2016). Unraveling the Effects of PPARβ/δ on Insulin Resistance and Cardiovascular Disease. Trends Endocrinol. Metab. *27*, 319–334.

Wang, Y.X., Lee, C.H., Tiep, S., Yu, R.T., Ham, J., Kang, H., and Evans, R.M. (2003). Peroxisome-proliferator-activated receptor δ activates fat metabolism to prevent obesity. Cell *113*, 159–170.

Wang, Y.X., Zhang, C.L., Yu, R.T., Cho, H.K., Nelson, M.C., Bayuga-Ocampo, C.R., Ham, J., Kang, H., and Evans, R.M. (2004). Regulation of muscle fiber type and running endurance by PPARdelta. PLoS Biol. *2*, e294.

Wang, X., Chrysovergis, K., Kosak, J., Kissling, G., Streicker, M., Moser, G., Li, R., and Eling, T.E. (2014a). hNAG-1 increases lifespan by regulating energy metabolism and insulin/IGF-1/mTOR signaling. Aging (Albany NY) *6*, 690–704.

Wang, X., Chrysovergis, K., Kosak, J., and Eling, T.E. (2014b). Lower NLRP3 inflammasome activity in NAG-1 transgenic mice is linked to a resistance to obesity and increased insulin sensitivity. Obesity (Silver Spring) *22*, 1256–1263.

Xu, X.Y., Nie, Y., Wang, F.F., Bai, Y., Lv, Z.Z., Zhang, Y.Y., Li, Z.J., and Gao, W. (2014). Growth differentiation factor (GDF)-15 blocks norepinephrine-induced myocardial hypertrophy via a novel pathway involving inhibition of epidermal growth factor receptor transactivation. J. Biol. Chem. *289*, 10084–10094.

Yang, L., Chang, C.C., Sun, Z., Madsen, D., Zhu, H., Padkjær, S.B., Wu, X., Huang, T., Hultman, K., Paulsen, S.J., et al. (2017). GFRAL is the receptor for GDF15 and is required for the anti-obesity effects of the ligand. Nat. Med. *23*, 1158–1166.

Zarei, M., Barroso, E., Leiva, R., Barniol-Xicota, M., Pujol, E., Escolano, C., Vázquez, S., Palomer, X., Pardo, V., González-Rodríguez, Á., et al. (2016). Heme-Regulated eIF2α Kinase Modulates Hepatic FGF21 and Is Activated by PPARβ/δ Deficiency. Diabetes *65*, 3185–3199.

STAR★METHODS

KEY RESOURCES TABLE

REAGENT OR RESOURCE	SOURCE	IDENTIFIER
Antibodies		
β-Actin	Sigma	A5441 RRID:AB_476744
AMPK	Cell Signaling	Cat#2532 RRID:AB_330331
Phospho-AMPK Thr^{172}	Cell Signaling	Cat#2531 RRID:AB_330330
ATF4 (CREB-2)	Santa Cruz	sc-390063 RRID:AB_2810998
eIF2α	Cell Signaling	Cat#9722 RRID:AB_2230924
ERK1/2 (p44/42 MAPK)	Cell Signaling	Cat#9102 RRID:AB_330744
Phospho-ERK1/2 (p42/44 MAPK) Thr^{202}/Tyr^{204}	Cell Signaling	Cat#9101 RRID:AB_331646
GAPDH	Millipore	MAB374 RRID:AB_2107445
GDF15	Santa Cruz	sc-515675 RRID:AB_2892674
Histone H3	Santa Cruz	sc-10809 RRID:AB_2115276
IκBα	Santa Cruz	sc-371 RRID:AB_2235952
Insulin receptor β	Cell Signaling	Cat#3025 RRID:AB_2280448
IRS-1	Cell Signaling	Cat#2382 RRID:AB_330333
Phospho-IRS-$1Ser^{307}$	Cell Signaling	Cat#2381S RRID:AB_330342
IRS-2	Cell Signaling	Cat#4502 RRID:AB_2125774
Lamin B	Santa Cruz	sc-6216 RRID:AB_648156
Lipin 1	Santa Cruz	sc-98450 RRID:AB_2135907
NF-κB p65	Santa Cruz	sc-109 RRID:AB_632039
p53	Cell Signaling	Cat#2524T RRID:AB_331743
Phospho-$p53Ser^{15}$	Cell Signaling	Cat#9284T RRID:AB_331464
PGC-1α	Abcam	ab54481 RRID:AB_881987
PPARα	Santa Cruz	sc-1985 RRID:AB_2165740
SOCS3	Santa Cruz	sc-9023 RRID:AB_2193305
STAT3	Santa Cruz	sc-482 X RRID:AB_632440
Phospho-$Stat3Tyr^{705}$	Cell Signaling	Cat#9131 RRID:AB_331586
Phospho-$Stat3Ser^{727}$	Cell Signaling	Cat#9134 RRID:AB_331589
α-Tubulin	Sigma	T6074 RRID:AB_477582
Chemicals, peptides and recombinant proteins		
A769662	Tocris Bioscience	3336
Compound C	Santa Cruz	sc-200689
GDF15	PeproTech	120-28
GDF15	R&D	8944-GD
GW501516	Sigma-Aldrich	SML1491
GW501516	Tocris Bioscience	5674
SB431542	PeproTech	3014193
Lipofectamine 2000	Thermo-Fisher	11668027
Pifithrin alpha p-nitro, cyclic (culture)	Millipore	506154
Pifithrin alpha p-nitro (*in vivo* treatment)	Santa Cruz	sc-222176
siRNA Control	Santa Cruz	sc-37007
siRNA PPARβ/δ	Santa Cruz	sc-36306
siRNA AMPK1/2	Santa Cruz	sc-45313
siRNA p53	Santa Cruz	sc-29436
siRNA GDF15	Santa Cruz	sc-39799

(*Continued on next page*)

Continued

REAGENT OR RESOURCE	SOURCE	IDENTIFIER
Critical commercial assays		
Mouse GDF15 ELISA Kit	Biorbyt	orb391081
Beta-Hydroxybutyrate Assay Kit	Sigma-Aldrich	MAK041
Experimental models: organisms/strains		
C57BL/6J mice	Envigo	5706M
C2C12	ATCC	CRL-1722
Software and algorithms		
Image Lab software (version 6.0.1)	Bio-Rad	https://www.bio-rad.com/en-us/product/image-lab-software
Graph Pad Prism 6.01	Graph Pad Software	https://www.graphpad.com/dl/96314/10B92408/

RESOURCE AVAILABILITY

Lead contact

Further information and requests for resources and reagents should be directed to and will be fulfilled by the lead contact, Manuel Vázquez-Carrera (mvazquezcarrera@ub.edu).

Materials availability

This study did not generate new unique reagents.

Data and code availability

The published article includes all datasets generated or analyzed during this study.

This paper does not report original code.

Any additional information required to reanalyze the data reported in this paper is available from the lead contact upon request.

EXPERIMENTAL MODEL AND SUBJECT DETAILS

Mice

Male C57BL/6 mice (10-12 weeks old) were purchased from (Envigo, Barcelona, Spain). Male *Gdf15*$^{-/-}$ mice (10-12 weeks old, C57BL/6/129/SvJ background) were gifts from Dr. Se-Jin Lee (Johns Hopkins University School of Medicine). Mice were housed and maintained under a constant temperature (22 ± 2°C) and humidity (55%). The mice had free access to water and food and were subjected to 12 h light-dark cycles. All experiments were performed in accordance with European Community Council directive 86/609/EEC, and experimental protocols as well as the number of animals, determined based on the expected effects size, were approved by the Institutional Animal Care and Use Committee at the University of Barcelona. Animal studies are reported in compliance with the ARRIVE guidelines (McGrath and Lilley, 2015).

Cell lines

Mouse C2C12 myoblasts (ATCC, Manassas, VA) were maintained in Dulbecco's modified Eagle's medium (DMEM) supplemented with 10% fetal bovine serum (FBS), 50 units/mL of penicillin and 50 mg/mL of streptomycin.

METHOD DETAILS

Animal treatments

After 1 week of acclimatization, the mice were randomly distributed into two experimental groups (n = 5 each), one of the groups receiving one daily oral gavage of vehicle (0.5% w/v carboxymethylcellulose) and the other one a daily oral dose of 3 mg/kg/day of GW501516 dissolved in the vehicle (volume administered 10 mL/kg) for 6 days. This dose has been reported to activate PPARβ/δ, but not PPARα or PPARγ (Lee et al., 2006). At the end of the treatment, the mice were sacrificed, and skeletal muscle (gastrocnemius) and liver samples were frozen in liquid nitrogen and then stored at −80°C. In a second study, mice were randomly distributed into three experimental groups (n = 5 each), one receiving one daily oral gavage of vehicle, one receiving a daily oral dose of 3 mg/kg/day of GW501516 for 6 days and one receiving GW501516 plus an intraperitoneal injection of the p53 inhibitor, pifithrin α *p*-nitro (2.2 mg/kg) dissolved in vehicle (PBS/DMSO, 10:1), every 48 h.

In a third study, male C57BL/6 mice (10-12 weeks old) were randomly distributed into four experimental groups (n = 5 each): (1) standard diet plus one daily oral gavage of vehicle (0.5% w/v carboxymethylcellulose); (2) Western-type high-fat diet (HFD, 45%

Kcal from fat, product D12451, Research Diets Inc., New Brunswick, NJ) plus one daily oral gavage of vehicle; (3) HFD plus one daily oral dose of 3 mg/kg/day of the PPARβ/δ agonist GW501516 dissolved in the vehicle; and (4) HFD plus one daily oral dose of 3 mg/kg/day of GW501516 dissolved in the vehicle (volume administered 10 mL/kg) for 3 weeks. Long-term treatment with this compound significantly reduces weight loss and fat mass (Wang et al., 2003, 2004), affecting both lipid metabolism and insulin sensitivity. To prevent the interference of weight loss in the parameters analyzed, mice were treated with the PPARβ/δ agonist for 3 weeks. Three days before the end of the 3-week treatment, mice in the first three experimental groups were injected once intraperitoneally with IgG (40 μg/mouse), while those in the fourth group received a neutralizing antibody (40 μg/mouse) against GDF15 (R&D Systems Inc., Minneapolis, MN) (Sasahara et al., 2017).

To evaluate the efficacy of the GDF15 neutralizing antibody we performed a fourth study where 12-week-old male C57BL/6J mice were randomly distributed into three different groups (n = 5), all receiving a standard diet. Mice were intraperitoneally injected with the GDF15 neutralizing antibody or IgG 48h before receiving 0.1 mg/kg of recombinant GDF15 or vehicle. The administration of recombinant GDF15 was performed at 18:00 h and measurement of food consumption was performed the next day at 8:00 h.

In a fifth study, male WT littermates controls and *Gdf15*$^{-/-}$ (10-12 weeks old, C57BL/6/129/SvJ background), obtained from Johns Hopkins University School of Medicine, were randomly distributed into three experimental groups (n = 5 each): (1) standard diet plus one daily oral gavage of vehicle (0.5% w/v carboxymethylcellulose); (2) Western-type high-fat diet (HFD, 45% Kcal from fat, product D12451, Research Diets Inc.) plus one daily oral gavage of vehicle; (3) HFD plus one daily oral dose of 3 mg/kg/day of the PPARβ/δ agonist GW501516 dissolved in the vehicle.

In the sixth study, male C57BL/6 mice (10-12 weeks old) were randomly distributed into two experimental groups (n = 5 each), one of the groups receiving two subcutaneous injections per day of saline and the other two subcutaneous injections of recombinant GDF15 (0.05 mg/kg), for two days. Mice were sacrificed two hours later after the last administration and skeletal muscle (gastrocnemius) samples were frozen in liquid nitrogen and then stored at −80°C.

For the glucose tolerance test (GTT), animals received 2 g/kg body weight of glucose by an intraperitoneal injection and blood was collected from the tail vein after 0, 15, 30, 60 and 120 min.

Liver histology

For histological staining studies, samples were formalin fixed, paraffin embedded and 4 μm sections obtained. Oil Red staining (Sigma Aldrich) was performed in 10 μm frozen liver sections. Fifteen images at 20x magnification were captured to quantify lipid droplets evaluated as the red stained area per total area with ImageJ software.

Cell culture

When C2C12 myoblasts reached confluence, the medium was switched to the differentiation medium containing DMEM and 2% horse serum, which was changed every other day. After 4 more days, the differentiated C2C12 cells had fused into myotubes. These were incubated in serum-free DMEM in either the absence (control cells) or presence of GW501516 (10 μM), A769662 (60 μM), compound C (30 μM) pifithrin-α (10 μM) or human GDF15 (100 ng/mL). Differentiated myotubes were transiently transfected with 70 nM siRNA against PPARβ/δ, AMPK1/2, GDF15 or p53 or siRNA control (Santa Cruz) in Opti-MEM medium (Thermo Fisher, MA) using Lipofectamine 2000 (Invitrogen, Carlsbad, CA) (7 μL per 1.5 mL well) according to the manufacturer's instructions. Different compounds were tested after 24 h of transfection.

Ex vivo skeletal muscle incubation

Soleus muscles were dissected in anesthetized mice, using isoflurane, and incubated *in vitro*, as previously described (Gumà et al., 1988) with some modifications as indicated following. The soleus muscles of each mouse were incubated in a single vial containing 4 mL of the incubation medium for a recovery period of 10 min at 34°C. After that, muscles were placed in new vials containing 3 mL of the incubation medium in the presence or absence of the respective treatments, GW501516 or recombinant mouse GDF15, for 90 min. Afterward, two consecutive replacements of the muscles were done in vials containing fresh medium and maintaining the respective treatments for a period of 90 and 60 min respectively, in order to favor the viability of the soleus muscles.

Reverse Transcriptase-Polymerase Chain Reaction and Quantitative Polymerase Chain Reaction

Isolated RNA was reverse transcribed to obtain 1 μg of complementary DNA (cDNA) using Random Hexamers (Thermo Scientific), 10 mM deoxynucleotide (dNTP) mix and the reverse transcriptase enzyme derived from the Moloney murine leukemia virus (MMLV, Thermo Fisher). The protocol was run in a thermocycler (BioRad) and consisted in a program with different steps and temperatures: 65°C for 5 min., 4°C for 5 min., 37°C for 2 min., 25°C for 10 min., 37°C for 50 min. and 70°C for 15 min. The relative levels of specific mRNAs were assessed by real-time RT-PCR technique in a Mini-48 well T100 thermal cycler (Bio-Rad) using SYBR Green Master Mix (Applied Biosystems), as previously described (Zarei et al., 2016). Briefly, samples contained a final volume of 20 μl, with 25 ng of total cDNA, 0.9 μM of primer mix and 10 μL of 2x SYBR Green master mix. The thermal cycler protocol for real time PCR included a first step of denaturation at 95°C for 10 min and 40 repetitive cycles with three steps for denaturation, primer annealing and amplification: 95°C for 15 s, 60°C for 30 s and 72°C for 30 s. Primers sequences were designed using the Primer-BLAST tool (NCBI), based on the full mRNA sequences to find optimal primers for amplification and evaluated with the Oligo-Analyzer tool (Integrated DNA Technologies) to ensure optimal melting temperature (Tm) and avoid the formation of homo/hetero-dimers or nonspecific structures that can

interfere with the interpretation of the results. The primer sequences were designed specifically spanning the junction between exons. Values were normalized to glyceraldehyde phosphate dehydrogenase (*Gapdh*) or adenine phosphoribosyltransferase (*Aprt*) expression levels, and measurements were done in triplicate. All expression changes were normalized to the untreated control. Primer sequences used for real-time RT-PCR are shown in Table S1.

Western blot analysis

Isolation of total protein extracts was performed as described elsewhere (Zarei et al., 2016). Proteins (30 μg) were separated by SDS-PAGE on 8%–12% acrylamide gels and transferred onto Immobilon polyvinylidene difluoride membranes (Millipore). Incubation with primary antibody was performed overnight in cold room in WestVisionTM Block and Diluent Solution (Cat. No: SP-7000, Vector Labs, CA), the membranes were washed five times with a TBS 0.1% tween solution and incubated with a horseradish peroxidase conjugated secondary antibody (GE Healthcare) in TBS 0.1% tween 3% BSA for one hour at room temperature. After incubation with the secondary antibody membranes were washed three times with a PBS 0.1% tween solution incubated with detection reagent. Protein bands were detected with the Western Lightning® Plus-ECL chemiluminescence kit (PerkinElmer, Waltham, MA). The size of the detected proteins was estimated using protein molecular mass standards (Bio-Rad, Barcelona, Spain). Signal acquisition was performed using the Bio-Rad ChemiDoc apparatus and quantification of immunoblot signal was performed with the Bio-Rad Image Lab software. The results for protein quantification were normalized to the levels of a control protein to avoid unwanted sources of variation.

QUANTIFICATION AND STATISTICAL ANALYSIS

Statistical analysis

Results are expressed as means ± s.e.m. of at least four independent experiments or at least four different animals per group. Results were analyzed by Student's t test or one-way analysis of variance (ANOVA), according to the number of groups compared, using the GraphPad Prism program (V8.4.3.) (GraphPad Software Inc., San Diego, CA). When significant variations were found by ANOVA, the Tukey-Kramer multiple comparison post hoc test was performed only if F achieved a P value < 0.05 and there was no significant variance in homogeneity. Differences were considered significant at $p < 0.05$. Specific statistical tests done for experiments are included in the figure legends.